The Mathematical Theory of SOC Systems with Applications to the Evolution of the Earth's Surface

IPAM Tutorials March 2008

Björn Birnir[1]
Center for Complex and Nonlinear Science
and
Department of Mathematics
University of California
Santa Barbara, CA 93106, USA

[1]and the University of Iceland, 107 Reykjavík, email: birnir@math.ucsb.edu

Chapter 1

Introduction

The evolution of the surface of the earth is a challenging and fascinating problem. Although the basic physical processes eroding the surface and moving the resulting sediment are understood, modeling them is in general very difficult. Not only can the surface consist of different types of material, rock, sand, soil and vegetation, most surfaces are also extremely complex both in composition and topography and over geological time tectonic uplift and earthquakes can have a profound effect on topography. Thus a basic problem in geomorphology is to model all of these different effects and then put them together in a mathematical model that can produce realistic landsurfaces. Such a model would give a valuable insight into the various forces that shape the surface and be a guide and a useful tool to geologists studying complex formations in geology.

The complexity of most landsurfaces and the instability of some raises a fundamental modeling question and a question of predictability. Should landsurfaces be modeled by physically based deterministic models, expressed as partial differential equations (PDEs), or should they by be modeled as stochastic particle systems (cellular automata) given the inherent influence of noise in the environment on these system? That noise is ubiquitous in landsurface evolution is clear when variations in rainfall rate, rock compositions and topography are considered. A

related question is what features of topography are predictable given some initial topography. It is known that realistic landsurfaces can be created by particle models using a random walk of water and sediment if they are seeded by quenched noise. However, this leaves something to be desired from a scientific perspective because one would like to understand the forces that play a role in the creation of the surface and what features of the surface are predictable and which are not.

Research on the evolution of river networks since the work of Horton [53] may be classified according to the class of model used. A first class of models based on *discrete modeling techniques*, these are analogous to models for phase transitions in statistical mechanics, has been remarkably successful in simulating the geometric and topological characteristics of stream networks [30, 31, 58, 2, 29, 32]. Many of these models, however, such as those used by Shreve [63, 64], illustrate how simple statistical approaches that essentially ignore physical mechanisms can give rise to good descriptions of many features of river networks. Such models typically provide little physical insight into the underlying phenomena. Researchers who attempt to incorporate physically-based mechanisms into discrete models have typically found it necessary to adopt strong assumptions concerning the initiation of channelized flows. The well-known model of Willgoose et. al. [30, 31], for example, employs two partial differential equations to determine two states: the first being surface elevation and the second an indicator variable of channelization. While the second variable and its governing equation lead to realistic simulations, it is difficult to relate either to well-established principles of fluid flow and erosion and hence there is some mistrust of the results of the model.

Another class of models has focused on the search for *variational principles* [1, 57, 27, 12] using both discrete and continuous modeling approaches. Such models have led to simulation results suggesting that fluvial networks may be governed by simple optimality principles. Sinclair and Ball [12], for example, recently indicated how local erosion rules lead to an optimality

principle. These approaches, however, do not provide adequate models of the emergence of channelized flows while the variational principles evoked are typically difficult to justify on physical grounds.

A third class of models is based on *continuous modeling techniques, conservation conditions, and constitutive relationships* expressed in terms of PDEs. Such models have led to (1) some understanding of early instabilities underlying the initiation of channelized flow [72, 37, 23, 24, 2, 73, 36]; (2) a significant understanding of the *mature* phases of drainage basin evolution [7, 71, 74]; (3) a rigorous derivation of variational principles governing drainage basin evolution [71]; and, quite recently, to (4) valuable insights into the emergence of channels and related scaling laws (see [11, 21, 22, 10] and below).

Developments in nonlinear, deterministic and probabilistic mathematics during the last two decades are now ripe for a new and powerful synthesis. These theories raise the prospect for advances in the geosciences that used to be out of reach of mathematical modeling and they are also leading to significant advances in the theory of nonlinear stochastic partial differential equations (SPDEs).

For a long time the unsurmountable problem in the theory of landsurface evolution was the role of noise and instabilities. Erosion is driven by small noise because both the eroding surfaces are unstable and small noise may trigger a large event. These instabilities will typically take the small noise that always exists in nature and in numerical computations and amplify it until it become large enough to drive the system. The most challenging problem is how highly colored the noise is when it comes through the magnifying glass created by the nonlinearities. The small noise in the surroundings and in computations may be white, or uniformly distributed in time and space, but the large noise that drives these systems is strongly colored, or non-uniform, both in space and time. In this paper we will investigate how noise is brought into the third class of models discussed above.

1.1 The Noise Creation

The details of the noise creation can be understood in roughly the following manner. The tiny perturbations caused by the small noise in the environment grow exponentially for a while because of the exponential growth created by the instabilities. But they do not grow exponentially forever as they would do if the system was linear. Instead the nonlinearities will saturate the exponential growth and instead one gets noisy terms that are no longer small. Moreover, since different modes get saturated in different ways and at different times, the large noisy terms are no longer white. They become colored in some way that is characteristic to the system. In turn this large colored noise will drive the system and create a characteristic noise-driven state.

The first conclusion we can draw from this argument is that evolving surfaces are not predictable. They are deterministic in the sense that the solutions are determined by the initial conditions and one can make infinite-dimensional mathematical models that describe them, but we cannot predict where the mountain or valley will be located or when the earthquake will occur and how big it will be. However, these processes possess statistical behaviors that are predictable. For example how rough the surface will be as specified by the variogram can be predicted. It is then appropriate to adopt the language of probability theory when discussing these system and think about their solutions as random variables that possess deterministic statistical properties.

The situation in geomorphology is in many respect analogous to the situation in chaotic dynamics some forty years ago. Then scientists were faced with problems that could be posed as initial value problems for ordinary differential equations (ODEs) but produced solutions that are not predictable due to sensitive dependence on initial conditions, or instabilities magnified so much by tiny random perturbations that predictability was lost. This is referred to as the *Butterfly Effect*. The difference is that whereas the ODE systems were finite-dimensional, landsurface erosion is an infinite-dimensional phenomenon, described by partial differential

equations (PDEs).

1.1.1 Ill-posed Problems

The infinite-dimensionality made erosion mathematically untouchable until recently. The reason was that the PDE initial value problems that one could pose in infinite-dimensions were ill-posed and this led researchers to the conclusion that these problems could not be solved, or at least not numerically. Indeed this is true for linear problems that are ill-posed in the strongest sense, because then the smallest modes will grow the fastest and after a short time the insignificant details represented by these modes will completely saturate any computation. More recently it has been realized that this is not the case for many ill-posed nonlinear problems. The reason is that although the smallest modes grow initially the fastest they are also saturated the fastest and simply end up contributing to the tail-end or high frequencies of the colored noise.

The numerical analysis of nonlinear SPDEs is still a formidable challenge and nonlinear PDEs accompanied by ill-posed problems that turn themselves into nonlinear SPDEs are even harder to solve. Not until recently has significant progress been made on how to solve such equations numerically. The first observation was that explicit methods that are the methods of choice for most computationally intensive problems because of their speed, were completely useless. These methods require a significant amount of artificial dissipation to be put in by hand. Whereas they can reproduce the large structures in the problems, they get the production of the colored noise wrong every time. Its characteristic structure (the color) is simply destroyed by the amount of artificial numerical viscosity. The numerical methods that produce the correct color are *implicit methods* [47], because although these methods also create numerical dissipation, it is much smaller and created in such a controlled fashion that it does not significantly alter the coloring of the noise. Thus implicit methods creating very small numerical dissipation capture the magnification of the noise by the instabilities and produce numerically

the stochastic processes with the correct statistical properties. The price one pays is that the resulting computations are very intensive, the implicit methods are much slower than the explicit ones, and to produce realistic landsurfaces and earthquakes on a fault system requires a large computational facility dedicated to these computations. This was another reason why earth scientists had not attempted such computations earlier; not until recently with the emergence of powerful Beowulf clusters of workstations have these large-scale parallel computations become economically feasible.

1.2 SOC Systems

The stochastic processes describing landsurface evolution are characterized by the statistical quantities associated to them. The evolution of the statistical quantities can be described in the following way. Initially they are not stationary but grow in time as a polynomial with a characteristic leading coefficient called the temporal roughness coefficient β. There is an equivalence between the spatial and the temporal scale given by another coefficient z called the dynamic coefficient coefficient, or $t \sim x^z$. Eventually the system reaches a critical size or feels the influence of the boundaries and the temporal roughening saturates into a statistically stationary state where the statistical quantities do not grow any more, but the system fluctuates about the statistically stationary state and the fluctuations are correlated. In this stationary state the statistical quantities are characterized by a polynomial scaling, given by the spatial roughness exponent χ. Only two of those exponents are independent because of the equivalence of the space and time scales. Their relationships is given by the equation,

$$\chi = \beta \cdot z. \tag{1.1}$$

The statistically stationary state is determined by an invariant measure living on infinite-

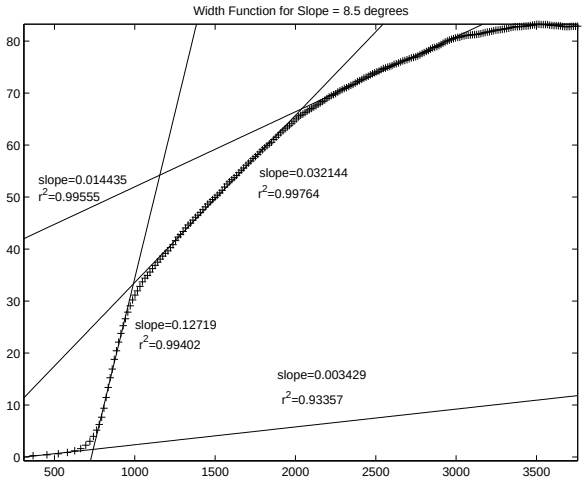

Figure 1.1: The scaling exponents of the variogram are shown as a function of time, for an initial landsurface with a slope of 8.5 degrees, on a log-log plot. The temporal evolution shows four different exponents (slopes), along with their regression coefficients, and a statistically stationary state (with slope zero) is emerging, furthest to the right.

dimensional phase space. This invariant measure determines a probability density that permits a computation of all the relevant statistical quantities and it is invariant with respect to the temporal evolution of the stochastic process. Typically the invariant measure lives on an infinite-dimensional subspace and the temporal roughening process projects the dynamics onto this infinite-dimensional subspace. If the invariant measure is *colored* so that the different directions, in the infinite-dimensional space occupied by the measure, have different weights then we will call the system *an SOC system*. Moreover, if the temporal roughening is characterized by more than one temporal roughening coefficient $\beta_k,\ k = 1,\cdots,n$, then the process is called *multi-fractal*. This means that there are statistical quantities whose rate of growth during the initial transient are not related. The multi-fractality is a signature of the complexity of the process and such systems will be called an SOC systems with *complex transients*.

In the physics literature SOC systems have been studied for a long time and go by the name of self-organized-critical system. The (somewhat vague) idea was that the system somehow self-organized during the initial transient and formed a ”SOC attractor” in the stationary state.

The mathematical theory developed for the landsurface evolution showed that no attractor except the trivial one exists but the system projects onto a subspace which is therefore attracting during the transients. Instead of an attractor there is an invariant measure living on this subspace and this invariant measure completely determines the statistically stationary state. The stationary state is critical in the sense that the motion is ergodic on the subspace and both large and small events are possible. Moreover their distribution is determined by the associated probability density.

The abundance of power laws in nature was noticed and studied by many authors during the 19th century, see for example Willis [80], Zipf [82] and Mandelbrot [46]. Many time-series including electrical noise and stock market price variation, for example, show power-law tails in their power spectra and this is called 1/f noise, see Press [52]. In 1987, Bak, Tang and Wiesenfeld [5, 6] proposed SOC as an explanation of the ubiquity of 1/f noise in nature. The book by Per Bak: How Nature Works : the science of self-organized criticality [3] contains many applications of SOC to natural phenomena.

We will now give a brief introduction to SOC from a physical point of view following Sneppen [67] and Dhar [16], with references for readers who want to read more of this literature. Bak, Tang and Wiesenfeld [5] observed that mountain ranges, river networks and coastlines have fractal structure, meaning that some correlation function has a power law behavior. For mountain ranges the correlation is the variogram (width function) that scales as a function of the lag variable, or the distance between two locations,

$$V(x,y,t) \sim |x-y|^{\chi}$$

with characteristic exponent χ, in the statistically stationary phase. The characteristic exponent takes the values $\chi = 0.5$ for channelizing surfaces, $\chi = 0.66$ for young surfaces and $\chi = 0.75$ for mature surfaces, in the transport-limited situation, see [10]. The width function played an

important role in the analysis of surface growth, see Kardar, Parisi and Zhang [38]. The shape of a river basin is determined by both its young and mature phases and the first and the third scaling laws above together produce Hack's law [34]. Hack's law says that the length of the main river in a river basin scales with the area of the river basin to the power 0.58, see [10]. Actually, the exponent in Hack's law has a range $0.5 - 0.7$ depending on whether the river basin is young our old, small or large, see [22, 18, 19, 20] for details. The ranges in Hack's law will be important for us below and we will associate them with three difference processes shaping landsurfaces, initial channelization, adolescent growth and maturation. Another example is the well-known Gutenberg-Richter law [33] for earthquakes. The interpretation of the existence of such a power law is that the system does not possess a characteristic scale instead all scales are connected. The absence of a characteristic scale means that the details of the system behavior are not important, instead statistical properties must be used to describe the system as a whole and these statistical properties should be scale invariant.

The SOC terminology originated in statistical mechanics where systems exhibiting correlations with power law decay over a wide range of length scales are said to have critical correlations. This is because correlations much larger than the length-scale of interactions were first studied in equilibrium statistical mechanics in the neighborhood of critical phase transitions. One needs to fine-tune some physical parameters (for example temperature and pressure) to specific critical values. In nature this is rather unlikely to happen for example the growth of a mountain range by uplift and its erosion is unlikely to be fine tuned to any parameters. The systems that we are interested in are not in equilibrium, there is variation in time but average properties are roughly constant in time. These system are frequently open and dissipative. We can for example think about the influences of uplift and rainfall on a mountain range and the balancing dissipation of sediment by erosion. Thus we consider these states to be *non-equilibrium steady states*.

Bak, Tang and Wiesenfeld argued that the dynamics which give rise to the robust power-law correlations seen in the equilibrium steady states in nature must not involve any fine-tuning of parameters. It must be such that the systems under their natural evolution are driven to a state at the boundary between the stable and unstable states. Such a state then shows long range spatio-temporal fluctuations similar to those in equilibrium critical phenomena. They also proposed a system whose natural dynamics drives it toward and then maintains it at the edge of stability: a sandpile. Their model was actually not a very good model for real sand, [35], however it was solvable and generated a large number of papers, see [75] and [15] for recent reviews. It also inspired experiments on piles of long-grained rice [28] that constitute an SOC system.

The sandpile model proposed by Bak, Tang and Wiesenfeld can be solved explicitly. This is of course very useful because it mean that various properties of the system can then be spelled out in all details. In [16] a slight generalization called the directed Abelian Sandpile Model (ADM) is solved and it is shown that ADM is equivalent to Scheidegger's model of river basins [62], Takayasu's aggregation model [68] and the voter model; see [45] and [25]. This means that all of these models occupy the same universality class with the same scaling exponents. In a recent paper Dhar and Mohanty [17] showed that the directed sandpile models fall in the same universality class as directed percolation; see [25].

We do something similar in this paper with the continuum models, namely solve the linear SPDEs driven by colored noise, see the next two sections, and spell out all their scaling laws. It will be clear that all scaling exponents in a reasonable range in one-dimension are possible. This means that there exist solvable SPDEs occupying all the available universality classes. Then we will see in our applications to the nonlinear landsurface equations that three universality classes are picked out by these nonlinear equations: one for the channelizing surfaces, another for young surfaces and the third for the mature ones. In a neighborhood of these surfaces the nonlinear landsurface equations occupy the same universality class as the corresponding

solvable linear SPDEs. It is obvious that our SOC systems are equivalent to the SOC systems in the physics literature because both are completely characterized by their scaling exponents.

1.2.1 Temporal scaling invariance

The statistical quantities characterizing the SOC systems have scaling invariances initially as functions of time and eventually as functions of space. In Figure 1.1 the temporal evolution of the variogram is shown as a function of time on a log-log plot. The figure shows that the temporal evolution grows polynomially and is characterized by several scaling exponents $\beta_k,\ k = 1,\cdots,4$ which are shown as the slopes on the lines fitting the numerical data. This implies that there exist several cross-over regions with different spatial scalings. The first characteristic exponent for the maturation process, see [10], is of the order $\beta_2 = 0.127$, which is in agreement with the theory, and the higher order exponents are smaller; eventually the graph levels off. This signifies that the system has entered the *statistically stationary state* that is characterized by the exponent $\beta_4 = 0$. The data is composed of an ensemble average over five numerical runs with an initial condition consisting of a smooth surface with a slope of 8.5 degrees, where each run is done with a different random seeding of the initial data. For each run the time evolution is averaged over the correlations of different spatial distances and a range of upslope positions. It is clear from the plot that the maturation process in landsurface evolution is multi-fractal in its temporal evolutions and eventually becomes stationary, different values of the initial slope produce similar results.

1.2.2 Complexity in Geomorphology

The evolution of the surface of the earth under the influence of tectonic uplift, weathering and erosion is a multi-scale multi-fractal process. In a series of papers Smith, Birnir and Merchant [71, 74, 65] developed a family of landscape models, based on the Smith-Bretherton model

[72], that capture the fundamental processes at work where landsurfaces are eroded by water. They showed that in numerical simulations these landscape models capture the emergence and development of stable, dendritic patterns of valleys and ridges. In a subsequent paper [10] they demonstrated the manner in which these models also capture the effects of random influences in driving the processes of landscape evolution. In particular, their results provided a physical basis for explaining various fundamental scaling relationships [44, 70, 55, 42, 60, 61, 59, 48, 54, 69, 62, 58, 32, 56, 21, 22] that characterize fluvial landscapes and supply a bridge between deterministic and stochastic theories of drainage basin evolution.

Birnir, Smith and Merchant [10] employed several specific techniques from the emerging theory of complex surface evolution (for a review see [41] and [8]) in investigating the models discussed in [71, 74] as systems driven by noise or stochastic processes. First, they characterized the statistical structure of eroding surfaces and flows in terms of various *structure functions* (or variogram) that represent the statistical correlation structure of complex surfaces. Second, they applied known results from this theory concerning the form of scalings that emerge from appropriate universality classes of PDEs when subjected to random driving forces of a specific form. The rationale for such application is that systems belonging to the same universality class manifest qualitatively similar behaviors. Birnir et al. also connected part of the theory to the concept of self-organized criticality (SOC) as proposed by Bak et al. [5, 6, 4, 49, 3, 67, 15, 16, 17].

Careful studies of Hack's exponent, see Dodds and Rothman [21, 22, 18, 19, 20], show that it has three ranges apart form very large and very small scale where the exponent is close to one. The three ranges seem to be shaped by a different type of water flow. The first range is characterized by the roughness coefficient $1/2$ of the water flow and corresponds to Brownian motion, see Edward and Wilkinson [26], of water over channelizing slopes, we will associate this range with the *Channelization Process*. The second range is associated with shock for-

mation, bores and hydraulic jumps in the water flow. It corresponds to quenched and pinned Burger's shocks, see Parisi [50] and Sneppen [66], and is characterized by the roughness coefficient $2/3$ of the water flow, see Welsh, Birnir and Bertozzi [78]. We will call this process of landsurfaces growing and evolving from a convex to a concave[1] shape the *Adolescence Process*. The largest range by far in Hack's exponent is associated with turbulent water flow, see Birnir [9], and is characterized by the scaling exponent $3/4$. We will associate this range with the *Maturation Process*.

[1]The use of these terms here and below follows their use in geomorphology which is opposite to the mathematical definition

Chapter 2

A Family of Landscape Evolution Models

The scaling results presented in this paper are derived from the same family of models studied analytically and numerically by Smith, Birnir, and Merchant [71, 74, 11]. These models represent the *advective entrainment and transport of sediment in transport limited* conditions [2]. Based on our previous analyses and on the results reported in this paper, we believe that they capture essential aspects of fluvial erosion at small to medium scales of spatial resolution [1]. While it is straightforward to extend these models to represent other processes that are significant in the evolution of fluvial landscapes, such as gravity-driven diffusion processes on hillslopes, we believe that their effects would mask the scaling relations associated with the advective processes of sediment transport in channel and overland flows [2].

We now provide a summary description of the family of models. A more detailed description of their derivation is provided in [71]. We also provide a brief discussion of those aspects of the characteristic time scales of the models that are relevant to the present context. The models are based on conditions describing the conservation of water and sediment fluxes over a continuous,

[1] Whether they capture essential aspects at large scales of spatial resolution is an open issue.
[2] We plan to explore the effects of such processes on scaling in later papers.

erodible surface $z = z(x,y,t)$

$$-R + \frac{\partial h}{\partial t} = \nabla \cdot (\mathbf{u}_w \, q_w), \tag{2.1}$$

$$\frac{\partial z}{\partial t} = \nabla \cdot (\mathbf{u}_w \, q_s) \tag{2.2}$$

in which $h = h(x,y,t)$ is the depth of water varying continuously over the landsurface, $-\mathbf{u}_w = -\frac{\nabla H}{|\nabla H|}$ is a unit vector in the direction of both water and the advected sediment flows, $H = H(x,y,t) = z(x,y,t) + h(x,y,t)$ is a free water surface, q_w represents the flux of water per unit width, and q_s represents the advected flux of sediment per unit width.

There are three natural time scales that characterize the dynamics of equations (2.1), (2.2). These time scales may be derived by transforming the variables of equations (2.1), (2.2) to dimensionless form, using relations $v = [v]v^*$ in which $[v]$ is a scale and v^* a dimensionless variable. Given values for the scaling parameters $[H], [h], [q_w], [q_s], [R]$ and $[x] = [y]$ that are characteristic of the variables in equations (2.1), (2.2), [3] we may then define representative values of the scaling parameter for the time variable ($[t]$) by setting the values of specific dimensionless parameters of the problem to unity.

A *short time scale* $[t]$ for t may be defined by the relation $[t][q_w]/[h][x] = 1$, which may be interpreted to imply that $[t]$ is the time scale at which the volume of water flowing over a lateral cross section of the ridge is approximately the same as the volume of water on the surface. Applying this scaling to dimensionless versions of equations (2.1), (2.2) and dropping the asterisks denoting dimensionless variables, we obtain

$$\frac{\partial h}{\partial t} = \nabla \cdot (\mathbf{u}_w \, q_w) + \frac{[x][R]}{[q_w]} R$$

[3] A useful set of such values characterize the representative scales when the basic model (2.1, 2.2) is used to represent the erosion of a small, linear ridge.

$$\frac{\partial H}{\partial t} - \frac{[h]}{[H]}\frac{\partial h}{\partial t} = \frac{[h][q_s]}{[H][q_w]}\nabla\cdot(\mathbf{u}_w\, q_s)\,.$$

It is natural to choose a scaling that makes the dimensionless parameter $[x][R]/[q_w] = 1$ in the water flow equation and interpret all terms in this equation as being $O(1)$ (see, for example, [**?**]). The significance of this fact, as we show in in Appendix in [10], is that the flows described by this equation are characterized by shock waves that we may interpret as short term noise. The order of the dimensionless parameter $[h][q_s]/[H][q_w]$ in the erosion equation is much smaller than unity and smaller than $[h]/[H]$. Hence we obtain the (approximate) erosion equation

$$\frac{\partial H}{\partial t} \approx \frac{[h]}{[H]}\frac{\partial h}{\partial t}$$

which indicates that variations in the water surface H are *small* at this time scale and driven by short term variations in the flow depth h described by the water flow equation. This equation also implies that erosion of the surface is negligible at this time scale.

A time scale $[t]$ that is *intermediate* between the previous short scale and longer scales may be defined by the relation $[t][q_s]/[h][x] = 1$, which implies that we may interpret $[t]$ as a time scale at which the volume of sediment flowing over a lateral cross section of the ridge is approximately equal to the volume of water on the ridge at any time. On applying this scaling to equations (2.1), (2.2) we obtain

$$\begin{aligned}\frac{[q_s]}{[q_w]}\frac{\partial h}{\partial t} &= \nabla\cdot(\mathbf{u}_w\, q_w) + R\\ \frac{\partial H}{\partial t} &= \frac{[h]}{[H]}\nabla\cdot(\mathbf{u}_w\, q_s) + \frac{[h]}{[H]}\frac{\partial h}{\partial t}\end{aligned}$$

where we have once more used the scaling relation $[x][R]/[q_w] = 1$. We note that the dimensionless parameter $[q_s]/[q_w]$ that multiplies the term $\frac{\partial h}{\partial t}$ has a magnitude that is greater than its magnitude at the short time scale. Since the evolution of the water surface H is determined

by two terms that we may assume to be $O(1)$ and since both are multiplied by the same small dimensionless parameter $[h]/[H]$, we may interpret this to mean that changes in the surface H are determined to a significant degree by small fluctuations in the depth of water h, indicated by the water flow equation, as well as by the erosion of the z surface.

A *long time scale* $[t]$ may be defined by the relation $[t][q_s]/[H][x] = 1$ and we may interpret $[t]$ as the time scale at which the volume of sediment flowing over a lateral cross section of the ridge represents a significant proportion of the volume of the ridge. On applying this scaling to equations (2.1), (2.2) and again using the scaling relation $[x][R]/[q_w] = 1$, we obtain

$$\begin{aligned} \frac{[h][q_s]}{[H][q_w]}\frac{\partial h}{\partial t} &= \nabla\cdot(\mathbf{u}_w\, q_w) + \frac{[x][R]}{[q_w]}R \\ \frac{\partial H}{\partial t} &= \nabla\cdot(\mathbf{u}_w\, q_s) + \frac{[h]}{[H]}\frac{\partial h}{\partial t}. \end{aligned}$$

The small size of the dimensionless parameter on the LHS of the water flow equation, $[h][q_s]/[H][q_w] \ll 1$, suggests that the basic flow is essentially an equilibrium flow down the surface gradient. It is not unreasonable, therefore, to adopt the following approximation to the water flow relation

$$0 \approx \nabla\cdot(\mathbf{u}_w\, q_w) + \frac{[x][R]}{[q_w]}R \tag{2.3}$$

as was done in the analyses in [72, 23, 71, 74]. While we may interpret the dominant balance in the erosion equation as being between the first two terms, we may interpret the relatively small term $[h]/[H]\partial h/\partial t$ as representing random variations that drive the sediment flow.

2.1 Previous Results for Long Time Scale Approximations

Smith, Birnir, and Merchant [71, 74] analyzed a subfamily of the models (2.1), (2.2) that was obtained with the use of the following assumption. First, the long time scale approximation

(2.3) to the basic model was assumed, together with the additional scaling relationship $[h]/[H] = [q_s]/[q_w] \equiv \eta$. Second, a Manning-type constitutive relation

$$q_w = nh^{\frac{5}{3}} |\nabla H|^{\frac{1}{2}} \tag{2.4}$$

where n, the inverse of the channel roughness, is a constant, was adopted to represent the flux of water. Third, a power law relation

$$q_s = kh^{\frac{5}{3}\gamma} |\nabla H|^{\frac{\beta}{2}+\delta} \tag{2.5}$$

was employed in representing the flux of sediment q_s. These assumptions lead to the following dimensionless equations:

$$-R = \nabla \cdot \left[\frac{\nabla H}{|\nabla H|} h^{\frac{5}{3}} |\nabla H|^{\frac{1}{2}} \right] \tag{2.6}$$

$$\frac{\partial H}{\partial t} - \eta \frac{\partial h}{\partial t} = \nabla \cdot \left[\frac{\nabla H}{|\nabla H|} h^{\frac{5}{3}\gamma} |\nabla H|^{\frac{\gamma}{2}+\delta} \right]. \tag{2.7}$$

The initial and boundary conditions employed in these analyses modeled a linear ridge undergoing erosion as a result of a uniform rainfall (see equations (4.1), (4.2) below.)

Applying the numerical methods described in [74] to equations (2.6)-(2.7), it was shown [74] that initially unstructured but randomly perturbed two-dimensional surfaces are unstable when eroded by water. Channelized flows develop on the surfaces with a region of maximum channelization first emerging towards the lower boundary of surfaces with an initially planar configuration [4]. This process of channelization involves the merging of "rivulets" and the for-

[4] A variety of numerical experiments have shown that channelization occurs on surfaces with a large array of

mation of larger "channels". The longitudinal profiles of the ridge simultaneously develop a concavity that also emerges initially near the base of the ridge under the influence of the fixed lower boundary. The region characterized by the maximum rate of channelization and by the emergence of the concavity gradually moves towards the upper boundary of the ridge as the surface erodes.

A pattern of dendritic valleys separated by ridges emerges and comes to dominate the eroding surface. Such a pattern is illustrated in Figures 1 and 2, which represent the surface after 10% of an initially planar surface has been eroded. After a characteristic period of erosion, the surfaces evolve towards stable landscapes of concave valleys and ridges that decay slowly in a self-similar manner. Such a pattern is illustrated in Figures 3 and 4, which represent the surface after 60% of an initial planar surface has been eroded [5].

The convergence to these forms occurs from initial surfaces that are both planar and non-planar. The characteristic period of erosion that precedes this convergence, which we measure in terms of the percentage of the original surface eroded, depends on the nature of the initial surface, the rainfall rate, and the parameters as γ and δ. These mature landscapes, consisting of stable patterns of concavities, valleys, ridges, and associated flows, are well-described by a class of solutions to the nonlinear PDEs (2.6)-(2.7) for cases in which $\eta \frac{\partial h}{\partial t}$ may be ignored in equation (2.7) relative to $\frac{\partial H}{\partial t}$ [71]. Such solutions depend on the characteristics of the water and sediment transport laws and on the boundary conditions for the PDEs; they are separable in time and space

$$H(x,y,t) = T_H(t)H_o(x,y), \quad h(x,y,t) = T_h(t)h_o(x,y); \tag{2.8}$$

initial configurations.

[5] We note, in particular, the sharpness of the longitudinal ridges, or divides, separating the valleys.

and they are stable [71]. They are also characterized in terms of a variational principle [71], by which a simple function of the sediment transport over the surface is minimized, subject to constraints involving the conservation of water flow and the elevations of the initial surface.

2.2 The Models Underlying the Present Analysis

The analysis presented in the current paper is similarly based on the use of equations (2.1), (2.2), the Manning-type constitutive relation (2.4) for the flux of water, a power law relation (2.5) for the flux of sediment, and the initial and boundary conditions prescribed in equations (4.3), (4.4). For reasons that we discuss below, however, *we no longer assume that the term* $\frac{\partial h}{\partial t}$ *in equation (2.1) is always negligible.* As we show this term leads to significant disturbances in the flow of water at the short time scales discussed in Section 2. We interpret these disturbances as noise, whose cumulative effects, as we discuss below, are significant in seeding the instabilities in the flow of sediment at the longer time scales.

We therefore focus our attention on the model

$$\eta^2 \frac{\partial h}{\partial t} = \nabla \cdot \left[\frac{\nabla H}{|\nabla H|} h^{\frac{5}{3}} |\nabla H|^{\frac{1}{2}} \right] + R, \tag{2.9}$$

$$\frac{\partial H}{\partial t} - \eta \frac{\partial h}{\partial t} = \nabla \cdot \left[\frac{\nabla H}{|\nabla H|} h^{\frac{5}{3}\gamma} |\nabla H|^{\frac{\gamma}{2}+\delta} \right] \tag{2.10}$$

in which we have adopted the scaling relation $[h]/[H] = [q_w]/[q_s] \equiv \eta$. In relation to the three time scales discussed above, we note that there is no loss of generality in this representation. In particular, we may obtain the short time scale version of the equations by applying the transformation $\tau = t/\eta^2$ and the intermediate time scale version by applying the the transformation

$\tau = t/\eta$.

We use the same boundary and initial conditions as [71, 74] to model a linear ridge extending uniformly in the lateral (x)-direction and defined over a rectangular domain of length L and width W,

$$D = \{(x,y) \in \mathbb{R}^2 | 0 \le x \le L,\ 0 \le y \le W\},$$

with initial conditions

$$\begin{aligned} h(x,y,0) &= d(y),\ d(0) = h_o,\ d(W) = 0, \\ H(x,y,0) &= cy + h_o,\quad 0 \le y \le W \end{aligned} \tag{2.11}$$

and boundary conditions

$$\begin{aligned} h(x,W,t) &= 0, \\ H(x,0,t) = &\quad h_0 \quad = h(x,0,t) \end{aligned} \tag{2.12}$$

corresponding to a water depth of zero at the top of the ridge and an absorbing body of water at the base of the ridge. While the water surface must be considered to be a free surface at the top of the ridge, it may be viewed as consisting of finitely many smooth curves that are solutions of a nonlinear ODE (the PDE restricted to the boundary). These curves are joined in a continuous, but not smooth, moving boundary (see, for example, Figure 3.) The upper boundary is characterized by the additional conditions

$$q_w = q_s = 0,$$

indicating the absence of any flux of water or sediment over this boundary. Since q_w and q_s are expressed as powers of h and ∇H in the constitutive relations, these conditions imply that the

vanishing of the water depth dominates the blow-up of the gradient of H (in q_w and q_s) and that the normal derivative of H may become infinite at the upper boundary

$$n \cdot \nabla H(x, w, t) = \infty.$$

The boundary conditions on the lateral boundaries of the ridge at $x = 0$ and $x = L$ are taken to be periodic, modeling a linear ridge of infinite extent.

Chapter 3

The Stochastic PDEs

We write the generic linear Stochastic PDE for SOC systems in the form

$$dU = \Delta U dt + dW, \quad x \in \Omega, \ t \in \mathbb{R}^+ \tag{3.1}$$

where $U(x,t)$ is the solution, Δ denotes the Laplacian and W is a Wiener process. We assume that Ω is either a box with periodic boundary conditions or a general domain with either Dirichlet or Neumann boundary condition. The initial condition is given by the formula

$$U(x,0) = u_0(x)$$

where $u_0(x)$ can either be a deterministic function or a stochastic process in x.

Now suppose that the Wiener process can be expressed as

$$W = \sum_{k=0}^{\infty} B_t^k e_k(x) \tag{3.2}$$

were the $B_t^n s$ are standard independent Brownian motions and the e_n are the eigenfunctions of the negative Laplacian $-\Delta$ on Ω with eigenvalues λ_n. Then the stochastic initial value problem

can be solved in the following manner. We seek a solution of the form

$$U(x,t) = \sum_{k=1}^{\infty} A_t^k e_k(x)$$

where the $A_t^n s$ are independent stochastic processes. A substitution into the stochastic PDE gives the stochastic ODE initial value problems

$$dA_t^k = -\lambda_k A_t^k dt + dB_t^k, \quad t \in \mathbb{R}^+$$

$$A_0^k = \hat{u}_0^k, \quad k = 0, 1, \ldots$$

These problems are easily solved

$$A_t^k = e^{-\lambda_k t} A_0^k + \int_0^t e^{-\lambda_k (t-s)} dB_s^k,$$

where the integral is the usual Ito's integral and the $A_t^n s$ are the so-called Ornstein-Uhlenbeck processes.

Now consider the stochastic initial value problem,

$$dU = \Delta U dt + dW$$

with periodic boundary conditions

$$U(x,t) = U(x + \hat{\imath}L, t); \quad U_x(x,t) = U_x(x + \hat{\imath}L, t), \quad t > 0,$$

where the $\hat{\imath}$ are unit vectors in $\mathbb{R}^n$ and initial conditions

$$u(x,0) = c, \quad 0 \le x_i \le L, \quad i = 1, .., n.$$

$W(dx,dt)$ now denotes a white noise process that is white in both space and time and characterized by its expectation

$$E(W(dx,dt)W(dx',dt')) = \delta(x-x')\delta(t-t')dxdx'dtdt'.$$

The solution of this initial value problem is

$$U(x,t) = c + \sum_{\substack{k=-\infty \\ k\neq 0}}^{\infty} A_t^k e_k(x).$$

where

$$A_t^k = \int_0^t \int_0^L \overline{e_k}(y) e^{-\lambda_k(t-s)} W(dy,ds), \quad k \in \mathbb{Z}^+,$$

and $\overline{e_k}$ denotes the complex conjugate of the basis function e_k. The basis functions are Fouries components (exponentials) because of the periodic boundary conditions.

Lemma 3.0.1

$$A_t^k = \int_0^t e^{-\lambda_k(t-s)} dB_s^k,$$

where B_t^k are standard, $\mathbb{R}$-valued independent Brownian motions.

Proof:

$$\mathrm{E}(A_t^k \overline{A_{t'}^{k'}}) = \int_0^t \int_0^L \int_0^{t'} \int_0^L \overline{e}_k(y) e_{k'}(y') e^{-\lambda_k(t-s)} e^{-\lambda_{k'}(t'-s')} \mathrm{E}\left(W(dy,ds)W(dy',ds')\right)$$

$$= \int_0^{t\wedge t'} \int_0^L \overline{e}_k(y) e_{k'}(y) dy \quad e^{-\lambda_k(t-s)} e^{-\lambda_{k'}(t'-s)} ds,$$

where $t \wedge t'$ denotes $min(t,t')$,

$$= \int_0^{t\wedge t'} e^{-\lambda_k((t+t')-2s)} ds, \qquad \text{if} \quad k = k',$$

and zero otherwise.

On the other hand,

$$\mathrm{E}\left(\int_0^t e^{-\lambda_k(t-s)}dB_s^k \cdot \int_0^{t'} e^{-\lambda_{k'}(t'-s')}dB_{s'}^{k'}\right) = \int_0^t \int_0^{t'} e^{-\lambda_k(t-s)}e^{-\lambda_{k'}(t'-s')}\mathrm{E}(dB_s^k dB_{s'}^{k'})$$

$$= \int_0^{t\wedge t'} e^{-\lambda_k((t+t')-2s)}ds, \qquad \text{if} \quad k = k',$$

and zero otherwise. Hence both sides of the equality represent zero mean Gaussian processes with same covariance function. **QED**

Now let E denote the expectation and V the width function or variogram, which is the square root of the second moment ρ_2,

$$V^2(x,y,t) = \mathrm{E}(|U(y,t) - U(x,t)|^2),$$

then, when the initial conditions are constant, we obtain

Lemma 3.0.2

$$E(A_t^k\overline{A_t^k}) = \frac{1-e^{-2\lambda_k t}}{2\lambda_k},$$

and

$$V^2(x,y,t) = \sum_{k=-\infty}^{\infty} \frac{1-e^{-2\lambda_k t}}{2\lambda_k}|e_k(y) - e_k(x)|^2.$$

Proof: Let $t = t'$ in the above proof to obtain

$$\mathrm{E}(A_t^k\overline{A_{t'}^{k'}}) = \int_0^t e^{-2\lambda_k(t-s)}ds = \frac{1-e^{-2\lambda_k t}}{2\lambda_k}.$$

The width function is computed in the following manner,

$$\mathrm{E}(|U(y,t)-U(x,t)|^2)=\sum_{k=-\infty}^{\infty}\sum_{j=-\infty}^{\infty}\mathrm{E}(A_t^k\overline{A_t^j})|e_k(y)-e_k(x)|^2,$$

since $\mathrm{E}(A_t^k\overline{A_t^j})=0$, if $k\neq j$, and otherwise by the formula above, this is equal to

$$\sum_{k=-\infty}^{\infty}\frac{1-e^{-2\lambda_k t}}{2\lambda_k}|e_k(y)-e_k(x)|^2.$$

QED

If the initial conditions are not constant they usually give a contribution to V.

The above formula for the width function is perfectly general but we will now specialize to one dimension and a domain that is an interval with periodic boundary conditions. In this case the basis of eigenfunctions of the Laplacian are the Fourier components with the following eigenvalues

$$e_k(x)=\frac{1}{\sqrt{L}}e^{\frac{2\pi ki}{L}x};\qquad \lambda_k=\left(\frac{2\pi k}{L}\right)^2;\qquad k\in\mathbb{Z}.$$

The estimates can be carried out in higher dimensions but the applications that we have in mind are to a one-dimensional width function. This means that we can identify the interval $[0,L]$ with periodic boundary conditions as the circle S^1. We let $a\wedge b$ denote the minimum of a and b. The following estimates are proven in Walsh [76]; see also Edward and Wilkinson [26].

Lemma 3.0.3 *The following two estimates hold*

$$\sum_{k=-\infty}^{\infty}\frac{1-e^{-2\lambda_k t}}{2\lambda_k}\leq\left(\frac{L}{2\pi}\right)^2\wedge\sqrt{t}\left(\frac{L}{\sqrt{2}\pi}+\frac{2\sqrt{2}\pi}{L}\right),$$

and

$$\sum_{k=-\infty}^{\infty} \frac{|e_k(y)-e_k(x)|^2}{2\lambda_k} \leq \frac{1}{\pi}|y-x|.$$

Proof:

$$1-e^{-2\lambda_k t} \leq 1$$

always holds. In particular if

$$t \geq \frac{1}{2}\left(\frac{L}{2\pi}\right)^2,$$

then it follows by the integral test that

$$2\sum_{k=1}^{\infty} \frac{1-e^{-2\lambda_k t}}{2\lambda_k} \leq 2\int_1^{\infty} \frac{1}{2\left(\frac{2\pi u}{L}\right)^2} du$$

$$= \left(\frac{L}{2\pi}\right)^2.$$

On the other hand, if

$$t < \frac{1}{2}\left(\frac{L}{2\pi}\right)^2,$$

then

$$2\sum_{k=1}^{\infty} \frac{1-e^{-2\lambda_k t}}{2\lambda_k} \leq \sum_{k=1}^{\infty} \frac{1}{\left(\frac{2\pi k}{L}\right)^2} \wedge 2t \leq 2\int_0^{\frac{1}{\frac{2\pi}{L}\sqrt{2t}}} t\,du + \int_{\frac{1}{\frac{2\pi}{L}\sqrt{2t}}}^{\infty} \frac{1}{u^2} du$$

$$= \frac{L\sqrt{t}}{\sqrt{2}\pi} + \frac{2\pi\sqrt{2}t}{L} \qquad \text{if,} \quad t \leq \frac{1}{2}\left(\frac{L}{2\pi}\right)^2.$$

The proof of the second inequality is

$$\left(\frac{e^{\frac{2\pi k i}{L}y}}{\sqrt{L}} - \frac{e^{\frac{2\pi k i}{L}x}}{\sqrt{L}}\right)\overline{\left(\frac{e^{\frac{2\pi k i}{L}y}}{\sqrt{L}} - \frac{e^{\frac{2\pi k i}{L}x}}{\sqrt{L}}\right)} = \frac{1}{L}\left(1 - e^{\frac{2\pi k i}{L}(y-x)} - e^{-\frac{2\pi k i}{L}(y-x)} + 1\right)$$

$$= \frac{4}{L}\sin^2\left(\frac{\pi k}{L}(y-x)\right) \leq \frac{4}{L}\left(1 \wedge \left(\frac{\pi k}{L}(y-x)\right)^2\right).$$

Therefore,

$$\sum_{k=-\infty}^{\infty} \frac{|e_k(y)-e_k(x)|^2}{2\lambda_k} \leq \sum_{k=1}^{\infty} \frac{2}{L} \frac{\left(1 \wedge \left(\frac{\pi k}{L}(y-x)\right)^2\right)}{\lambda_k}$$

$$= \frac{2}{L}\sum_{k=1}^{\infty} \frac{1}{\left(\frac{2\pi k}{L}\right)^2} \wedge \frac{(y-x)^2}{4} \leq \frac{1}{2}\int_0^{\infty} \frac{L}{\pi^2 u^2} \wedge \frac{(y-x)^2}{L} du$$

$$= \frac{1}{2}\int_0^{\frac{L}{\pi|y-x|}} \frac{(y-x)^2}{L} du + \frac{1}{2}\int_{\frac{L}{\pi|y-x|}}^{\infty} \frac{L}{\pi^2 u^2} du = \frac{1}{2}\left(\frac{|y-x|}{\pi} + \frac{|y-x|}{\pi}\right)$$

$$= \frac{1}{\pi}|y-x|.$$

QED

The width function characterizes both an initial transient state and a stationary state for the stochastic process $U(x,t)$, these two different states are characterized by t (temporal) and x (spatial) scalings of the width function.

Theorem 3.0.1 *The stochastic process defined by the equation (3.1) and the noise (3.2) possesses both a transient and a stationary state. Initially, during a transient growth,*

$$V(x,y,t) \leq \frac{\sqrt{2}}{\sqrt{L}}\left[\left(\frac{L}{2\pi}\right) \wedge \left(\frac{L}{\sqrt{2}\pi} + \frac{2\sqrt{2}\pi}{L}\right)^{1/2} t^{\frac{1}{4}}\right]$$

whereas in the stationary state

$$V(x,y,t) \leq \sqrt{\frac{1}{\pi}}|y-x|^{\frac{1}{2}}.$$

Proof: From Lemma 2.2,

$$V^2(x,y,t) = \frac{4}{L}\sum_{k=-\infty}^{\infty}\frac{1-e^{-2\lambda_k t}}{2\lambda_k}\sin^2\left(\frac{\pi k}{L}(y-x)\right) \leq \frac{4}{L}\sum_{k=-\infty}^{\infty}\frac{1-e^{-2\lambda_k t}}{2\lambda_k}.$$

The result follows from Lemma 2.3. The second estimates also follows from Lemma 2.3 and the trivial estimate

$$V^2(x,y,t) \leq \frac{4}{L}\sum_{k=-\infty}^{\infty}\frac{1}{2\lambda_k}\sin^2\left(\frac{\pi k}{L}(y-x)\right).$$

QED

Theorem 3.0.2 *There exists a Gaussian invariant measure*

$$\mu(dx) = exp\{-\sum_{-\infty}^{\infty}\lambda_k x_k^2 + \theta_k\}dx = \prod_{k=-\infty}^{\infty}\left(\frac{e^{-\lambda_k x_k^2}}{\sqrt{\pi/\lambda_k}}\right)dx_k$$

on the phase space $H = L^2(S^1)$, where $x = \sum_{k=-\infty}^{\infty} x_k e_k$ is a general vector in H, where $\theta_k = \frac{1}{2}\ln(\frac{\lambda_k}{\pi})$ is the normalization factor of the Gaussian.

The proof of Theorem 3.0.2 is a special case of the proof of Theorem 3.1.2 and Corollary 3.1.2.

3.1 SOC Systems

We will now define processes that we call SOC systems or SOC processes.

Definition 3.1.1 *A stochastic process U is an SOC system if it possesses both a transient growth state and a statistically stationary state satisfying the following four conditions:*

1. *The process possesses a scaling, so the width function $V = \rho_2^{\frac{1}{2}}$ scales with a temporal roughness exponent β during the initial transients and the spatial roughness exponent χ in the statistically stationary state.*

2. *There is an equivalence of time and space $t \sim |x|^z$ given by the temporal coefficient z*

$$\chi = z\,\beta$$

and the systems possesses a spatial scale L (system size, upper cut-off, wavelength selection) that is an upper limit for the spatial scaling. A lower limit for the length of the time-transients is given by $t \sim L^z$.

3. *The process projects the dynamics to a subspace H' of the original phase space H as $t \to \infty$. $H' = H$ is also permitted as a special case.*

4. *There exists an measure μ on this subspace H' and the process restricted to the subspace is invariant with respect to this measure.*

5. *The invariant measure is colored; that is: the infinitely many directions in H' are weighted (colored), with weights different from a pure Gaussian or Poissonian measure.*

The point of Condition 5 is that the invariant measure cannot be a pure Gaussian as in Theorem 3.0.2. However, it can be a weighted Gaussian as in Corollary 3.1.2 with the weights c_k providing the color. In general it will be a non-Gaussian or Poissonian measure that is colored in the above sense.

Definition 3.1.2 *An SOC process has* complex transients *if the process is multi-fractal during the initial transients, so that either the width function scales with several different rationally independent exponents, or homogeneous linear combinations of the higher moments $(\sum_{k=1}^{n} a_k \rho_k^{n/k})^{\frac{1}{n}}$, $n > 2$, scale with exponents β_n, which are rationally independent of β, $\beta_n \neq \frac{p}{q}\beta$, $p, q \in \mathbb{N}$.*

Definition 3.1.3 *An SOC process has a* complex stationary state *if the stationary state of the process is multi-fractal, so that homogeneous linear combinations of the higher moments $(\sum_{k=1}^{n} a_k \rho_k^{n/k})^{\frac{1}{n}}$,*

$n > 2$, scale with exponents χ_n, which are rationally independent of χ, $\chi_n \neq \frac{p}{q}\chi$, $p,q \in \mathbb{N}$, in the stationary state.

Example 3.1.1 We now solve the equation (3.1) with the *colored noise*,

$$dW = \sum_{k=0}^{\infty} c_k^{\frac{1}{2}} e^{-\alpha_k t} dB_t^k e_k(x). \tag{3.3}$$

Here the coefficients give different weight to the different directions e_k and represent *spatial coloring* whereas the exponential factors $e^{-\alpha_k t}$ give (an exponential) *temporal* coloring. Then by a similar computation as in Lemma 3.0.2

$$\mathrm{E}(A_t^k \overline{A_t^k}) = e^{-2\alpha_k t} \frac{1 - e^{-2(\lambda_k - \alpha_k)t}}{2(\lambda_k - \alpha_k)},$$

and the width function becomes

$$V^2(x,y,t) = \sum_{k=0}^{\infty} c_k e^{-2\alpha_k t} \frac{1 - e^{-2(\lambda_k - \alpha_k)t}}{2(\lambda_k - \alpha_k)} |e_k(y) - e_k(x)|^2.$$

The following estimates hold

$$V^2 \leq C t^{2\beta},$$

where $\beta = sup\ \beta'$ such that

$$\sum_{k=0,\ \alpha_k \neq 0}^{\infty} \frac{c_k}{|\lambda_k - \alpha_k|^{1-2\beta'}} < \infty, \tag{3.4}$$

C a constant and

$$V^2 \leq C\,|y-x|^{2\chi},$$

where $\chi = sup\ \chi'$ such that

$$\sum_{k=0,\ \alpha_k = 0}^{\infty} \frac{c_k}{\lambda_k^{1-\chi'}} < \infty. \tag{3.5}$$

The proofs are similar to the ones in Lemma 3.0.3.

An example of a noise that gives a process with the above scalings is the noise (3.3) with the coefficients, $c_k = \frac{a}{k^p},\ p = 2\chi - 1$, and $|\lambda_k - \alpha_k| = b\ k^q$, $q = \frac{2(1-\chi)}{1-2\beta}$, a and b being constants.

Colored Wiener processes with spatial coloring as in example 3.1 have been widely studied in the literature; see for example Dawson and Salehi [14] where they are used to describe random environments, and [51]. Dawson [13] gives a good account of linear PDEs driven by both white and colored noise. In particular, it is shown in these references that colored noise gives colored scalings for linear SPDEs.

We can now show that the stochastic process with the colored noise in Example (3.1) is an SOC process whereas the process defined by equation (3.1) and white noise (3.2) is not an SOC process.

Lemma 3.1.1 *The stochastic process in Example (3.1), defined by equation (3.1) with the colored noise (3.3), is an SOC process. Moreover, if* $\frac{1}{q}$ *is not a rational multiple of* β *then the stochastic process has complex transients.*

Proof: Conditions 1 and 2 in Definition 3.1.1 are proven by Example 3.1, L can here be taken to be the spatial period (system size). The third condition in Definition 3.1.1 is also proven in Example 3.1 which shows that as $t \to \infty$ the variance of U vanished except on the subspace where $\alpha_k = 0$. Since the mean of U also decays exponentially we see that the process is projected onto this subspace, $\alpha_k = 0$, where the statistically stationary state lives, see Example 3.1. Corollary 3.1.2 gives the existence of an invariant measure on this subspace and satisfies Condition 4 of Definition 3.1.1. Since this measure is a weighted Gaussian it also satisfies Condition 5. We need to show that with the conditions on β and q the process satisfies Definition 3.1.2. We will compute the fourth moment,

$$\rho_4 \quad = \quad \sum_{k=0}^{\infty} c_k^2 e^{-4\lambda_k t} \frac{(1 - e^{-2(\lambda_k - \alpha_k)t})^2}{4(\lambda_k - \alpha_k)^2} |e_k(y) - e_k(x)|^4$$

$$+ \quad 3\left(\sum_{k=0}^{\infty} c_k e^{-2\alpha_k t}\frac{1-e^{-2(\lambda_k-\alpha_k)t}}{2(\lambda_k-\alpha_k)}|e_k(y)-e_k(x)|^2\right)^2.$$

The second part of this expression scales as $t^{4\beta}$ by Equation 3.4 when t is small, the first part is estimated as in Example 3.1. By the integral test

$$\begin{aligned}\sum_{k=0,\ \alpha_k\neq 0}^{\infty} c_k^2 e^{-4\alpha_k t}\frac{(1-e^{-2(\lambda_k-\alpha_k)t})^2}{4(\lambda_k-\alpha_k)^2} &\leq \sum_{k=0,\ \alpha_k\neq 0}^{\infty} c_k^2\frac{1}{4(\lambda_k-\alpha_k)^2}\wedge t^2\\ &\leq C'\left(\int_0^{\frac{c}{t^{1/q}}} t^2\frac{1}{u^{2p}}du+\int_{\frac{c}{t^{1/q}}}^{\infty}\frac{1}{u^{2(p+q)}}du\right),\end{aligned}$$

assuming that $c_k=\frac{a}{k^p}$ and $|\lambda_k-\alpha_k|=\frac{b}{k^q}$, where C', a and b are constants. The last integral equals

$$= C'(\frac{1}{1-2p}+\frac{1}{2(p+q)-1})t^{\frac{2(p+q)-1}{q}} = Ct^{4\beta+\frac{1}{q}},$$

where $2\beta = 1+\frac{p-1}{q}$ and C is another constant. This shows that $(\rho_4-3\rho_2^2)^{1/4}$ scales with the exponent $\beta+\frac{1}{4q}$, which is rationally independent of β. **QED**

It is clear that the stochastic process in Example (3.1) does not have a complex stationary state, because its invariant measure on H' is a weighted Gaussian by Corollary 3.1.2. This implies that its variance and all homogeneous linear combinations of the higher moments scale with the same exponent given by (3.5).

Corollary 3.1.1 *The Edward-Wilkinson stochastic process defined by equation (3.1), with white noise (3.2), does not have complex transients, and is not an SOC process.*

Proof: The scaling $\beta=\frac{1}{2}$ corresponds to the long time asymptotics of Brownian motion and it is well know that the moments scale as $\rho_{2k}\sim t^k$ in that case. The Edward-Wilkinson process is the transient toward a Brownian motion and then the scaling of the second moment is $V^2=\rho_2\sim t^{1/2}$. The same argument as in the proof of the Theorem 3.0.1 gives the formula $\rho_{2k}\sim t^{k/2}$

for the initial transients. Thus no linear combination of the moments can scale with an exponent rationally independent of $\beta = \frac{1}{4}$. It is also easy to check by carrying the computation in Lemma 3.0.3 out for the higher order terms in t, that all the terms scale with the exponent $\frac{1}{4}$. Thus no other exponents appear in the scaling of V. This violates Definition 3.1.2. Conditions 1 and 2 of Definition 3.1.1 are satisfied by Theorem 3.0.1 and Theorem 3.0.2 gives an invariant measure supported on the full space ($H' = H$) and satisfies Conditions 3 and 4. However, it is a pure unweighted Gaussian measure and thus fails Condition 5. **QED**

Polynomial Colored Noise

In this section we will consider processes that are colored by polynomially decaying noise instead of exponentially decaying noise as in the last section. This is the coloring that we will encounter in the application to fluvial landscapes in the following sections. As always we consider a linear SPDE for a systems in the form

$$dU = \Delta U\,dt + dW, \quad x \in \Omega,\ t \in \mathbb{R}^+ \tag{3.6}$$

where $U(x,t)$ is the solution, and Δ denotes the Laplacian. We assume again that Ω is either a box with periodic boundary conditions or a general domain with either Dirichlet or Neumann boundary condition. The initial condition is given by the formula

$$U(x,0) = u_0(x)$$

where $u_0(x)$ can either be a deterministic function or a stochastic process in x.

We are now going to assume that the noise process is colored both in space and time and can be express as

$$dW = \sum_{k=0}^{\infty} c_k^{\frac{1}{2}} (t+t_0)^{-\alpha_k} dB_t^k e_k(x), \tag{3.7}$$

were the $B_t^n s$ are standard independent Brownian motions and the e_n are the eigenfunctions of the negative Laplacian $-\Delta$ on Ω with eigenvalues λ_n. Notice that this time-coloring of the noise is different from (3.3). There the noise decayed exponentially in time whereas here the decay is polynomial. Then the stochastic initial value problem can be solve in the following manner. We seek a solution of the form

$$U(x,t) = \sum_{k=0}^{\infty} A_t^k e_k(x)$$

where the $A_t^k s$ are independent stochastic processes. A substitution into the stochastic PDE gives the stochastic ODE initial value problems

$$dA_t^k = -\lambda_k A_t^k dt + c_k^{\frac{1}{2}} (t+t_0)^{-\alpha_k} dB_t^k, \;\; t \in \mathbb{R}^+$$

$$A_0^k = \hat{u}_0^k, \;\; k = 0, 1, \ldots$$

These problems are easily solved

$$A_t^k = e^{-\lambda_k t} A_0^k + c_k^{\frac{1}{2}} \int_0^t (s+t_0)^{-\alpha_k} e^{-\lambda_k (t-s)} dB_s^k,$$

where the integral is the usual Ito's integral but now the $A_t^k s$ are no longer Ornstein-Uhlenbeck processes.

Lemma 3.1.2 *Let*

$$Q_t^k = c_k \int_0^t (s+t_0)^{-2\alpha_k} e^{-2\lambda_k (t-s)} \, ds,$$

then

$$V^2(x,y,t) = \sum_{k=0}^{\infty} Q_t^k |e_k(y) - e_k(x)|^2.$$

The proof of the Lemma is similar to the proof of Lemma 3.0.2.

Lemma 3.1.3 *If* $\alpha_k \neq 0$, *then*

$$\lim_{t\to\infty} Q_t^k = 0.$$

Proof:

$$\lim_{t\to\infty} Q_t^k = c_k \lim_{t\to\infty} \int_0^t (s+t_0)^{-2\alpha_k} e^{-2\lambda_k(t-s)} ds.$$

The last integral is of the form

$$\int_0^t \frac{e^{-b(t-s)}}{(s+t_0)^a} ds = -\int_0^t \frac{e^{-bz}}{(t+t_0-z)^a} dz,$$

by the change of variables $z = t-s$. The integral on the right hand side of the last equation can be split

$$\int_0^\tau \frac{e^{-bz}}{(t+t_0-z)^a} dz + e^{-b\tau} \int_0^{t-\tau} \frac{e^{-bx}}{(t+t_0-x-\tau)^a} dx,$$

making the change of variables $z = x+\tau$ in the latter integral. Now the first integral converges uniformly and we can take the limit $t \to \infty$ inside the integral. The second integral converges and we can let $\tau = t/2$, then the second expression vanishes as $t \to \infty$ because of the decay of the exponential $e^{-bt/2}$ in front of the integral. Now let $\tau_k = t_k/2$ and $t > t_k \to \infty$, then both expressions converge to zero. **QED**

Lemma 3.1.4 *The following two estimates hold*

$$\sum_{k=0,\ \alpha_k\neq 0}^{\infty} Q_t \leq C t^{2\beta},$$

where

$$\beta = min_{n,k}(\frac{n}{2} - \alpha_k)_+, \ n \in \mathbb{Z}^+, \ k \in \mathbb{Z}^+,$$

where $(\cdot)_+$ *denotes the positive part, and*

$$\sum_{k=0,\ \alpha_k=0}^{\infty} \frac{c_k}{2\lambda_k} |(e_k(y) - e_k(x)|^2 \leq C\,|y-x|^{2\chi},$$

where $\chi = sup\ \chi'$ *such that*

$$\sum_{k=0,\ \alpha_k=0}^{\infty} \frac{c_k}{\lambda_k^{1-\chi'}} < \infty.$$

Proof: We integrate by parts to get

$$\sum_{k=0,\ \alpha_k\neq 0}^{\infty} Q_t^k = \sum_{n=1} \sum_{k=0,\ \alpha_k\neq 0} \frac{(2\lambda_k)^{n-1} c_k}{\prod_{j=1}^{n}(j-2\alpha_k)} t^{(n-2\alpha_k)}, \tag{3.8}$$

up to terms of higher order in t. For t small the fastest growing terms has the coefficient $\beta = min_{n,k}(n-2\alpha_k)$. If only finitely many α_ks satisfy, $\alpha_k \neq 0$, the sum converges. If infinitely many $\alpha_k \neq 0$ we can only integrate by parts as long as

$$\sum_{k=0,\ \alpha_k\neq 0} (2\lambda_k)^{n-1} c_k < \infty.$$

The proof of the second estimate is the same as in Example 3.1.1 using that $\lim_{t\to\infty} Q_t^k = 0$ for $\alpha_k \neq 0$ by Lemma 3.1.3. **QED**

Theorem 3.1.1 *The stochastic process defined by Equation (3.6) and the colored noise (3.7) possesses both a transient and a stationary state. Initially, during the transient growth,*

$$V(x,y,t) \leq Ct^{\beta},$$

C a constant, whereas in the stationary state

$$V(x,y,t) \leq C\,|y-x|^{\chi},$$

where the coefficients β *and* χ *are defined in Lemma 3.1.4.*

The following theorem is stated and proven as Theorem 6.2.1 in [51].

Theorem 3.1.2 *Consider the stochastic PDE (SPDE)*

$$dU = AU(t)dt + B(t)dW(t), \quad U(0) = x,$$

and suppose that A is the generator of a strongly continuous semi-group $S(t)$ *on a Hilbert space* H*, and* $B(\cdot)$ *a linear operator* $B : H \to H$*. For any* $t > 0$ *and* $x \in H$ *let*

$$Q_t = \int_0^t S(s)B(s)B^*(s)S^*(s)x\,ds$$

be a trace class operator. Then for any $x \in H$ *the solution* $U(t)$ *is a stochastic process* $\mathcal{P}(S(t)x, Q_t)$*, with mean* $S(t)x$ *and variance* Q_t *and the SPDE possesses an invariant measure, given by*

$$\nu * \mathcal{N}(0, Q_\infty)$$

where

$$Q_\infty = \int_0^\infty S(s)B(s)B^*(s)S^*(s)x\,ds$$

and ν *is the invariant measure of the deterministic PDE,* $u_t = Au$*.*

Proof: The assumption on A and B imply that

$$U(t) = S(t)x + \int_0^t S(t-s)B(s)dW(s)$$

is a mild solution of the SPDE.

The transition semi-group on H corresponding to the SPDE is

$$R_t\varphi(x) = \int_H \varphi(y)\mathcal{P}(S(t)x, Q_t)(dy)$$

A probability measure $\mu \in \mathcal{M}(H)$, $\mathcal{M}(H)$ is the set of all probability measures on H, is *invariant* if

$$\int_H R_t\varphi(x)d\mu(x) = \int_H \varphi(x)d\mu$$

for all bounded φ on H.

Now the simplest way to proceed is to consider the characteristic functional $\hat{\mu}$ of the measure $\mathcal{P}$,

$$R_t e^{i<h,x>} = e^{<h,S(t)x>}e^{-\frac{1}{2}<Q_t h,h>},\ x \in H,$$

for a fixed $h \in H$. We have let $\varphi(x) = e^{i<h,x>}$ and the computation is standard. Clearly this implies that μ is invariant if and only if

$$\hat{\mu}(h) = e^{-\frac{1}{2}<Q_t h,h>}\hat{\mu}(S^*(t)h). \tag{3.9}$$

It is this condition that we now prove. We define the measure to be

$$\mu(dx) = e^{-\frac{1}{2}<Q_\infty^{-1/2}x,Q_\infty^{-1/2}x>}dx,$$

so that

$$\hat{\mu}(h) = e^{-\frac{1}{2}<Q_\infty h,h>}.$$

Thus

$$\hat{\mu}(S^*(t)h) = e^{-\frac{1}{2}<Q_\infty S^*(t)h,S^*(t)h>} = e^{-\frac{1}{2}<S(t)Q_\infty S^*(t)h,h>}$$

where $h \in H$ and

$$S(t)Q_\infty S^*(t)h = -\frac{1}{2}Q_t h + \frac{1}{2}Q_\infty h$$

and substituting this expression in for $S(t)Q_\infty S^*(t)$ in the exponential

$$e^{-\frac{1}{2}<S(t)Q_\infty S^*(t)h,h>} = e^{\frac{1}{2}<Q_t h,h>} e^{-\frac{1}{2}<Q_\infty h,h>}$$

gives

$$\hat{\mu}(S^*(t)h)e^{-\frac{1}{2}<Q_t h,h>} = \hat{\mu}(h)$$

which is Condition (3.9).

QED

Corollary 3.1.2 *Let H' denote the subspace $\{x' = \sum_{k=0,\ \alpha_k=0} x_k e_k\}$. There exists a weighted Gaussian invariant measure*

$$\mu(dx') = exp\{-\sum_{k=0,\ \alpha_k=0} \frac{\lambda_k}{c_k}x_k^2 + \theta_k\}dx' = \prod_{k=0,\ \alpha_k=0}^{\infty} \left(\frac{e^{-\frac{\lambda_k x_k^2}{c_k}}}{\sqrt{\pi c_k/\lambda_k}} \right) dx_k$$

on H', where $\theta_k = \frac{1}{2}\ln(\frac{\lambda_k}{\pi c_k})$ is the normalization factor of the Gaussian.

Proof: Let H' be the subspace of H, $H' = \{x' = \sum_{k=0,\ \alpha_k=0} x_k e_k\}$. We need to proof Condition (3.9). In the proof of Theorem 3.1.2 we defined the measure to be

$$\mu(dx') = exp\{-\sum_{k=0,\ \alpha_k=0} \frac{\lambda_k}{c_k}x_k^2\}dx' = e^{-\frac{1}{2}<Q_\infty^{-1/2}x', Q_\infty^{-1/2}x'>}dx',$$

so that

$$\hat{\mu}(h') = e^{-\frac{1}{2}<Q_\infty h', h'>},$$

and Condition (3.9) becomes

$$\hat{\mu}(h') = e^{-\frac{1}{2}<Q_t h', h'>} \hat{\mu}(S^*(t)h').$$

Here the operator Q_∞ is defined by

$$Q_\infty x = \sum_{k=0,\ \alpha_k=0} \frac{c_k}{2\lambda_k} x_k e_k,$$

the $x_k s$ being the Fourier coefficients of $x = \sum_{k=0}^{\infty} x_k e_k \in H$. Thus

$$\hat{\mu}(S^*(t)h') = e^{-\frac{1}{2}<Q_\infty S^*(t)h', S^*(t)h'>} = e^{-\frac{1}{2}<S(t)Q_\infty S^*(t)h', h'>}$$

where $h' \in H'$ and

$$S(t)Q_\infty S^*(t)h' = \sum_{k=0,\ \alpha_k=0} \frac{c_k}{2\lambda_k} e^{-2\lambda_k t} h_k e_k = \sum_{k=0,\ \alpha_k=0} \frac{c_k}{2\lambda_k} (e^{-2\lambda_k t} - 1) h_k e_k + \sum_{k=0,\ \alpha_k=0} \frac{c_k}{2\lambda_k} h_k e_k,$$

where $h = \sum_{k=0}^{\infty} h_k e_k$ is the Fourier expansion of h. The last expression above is nothing but

$$-\frac{1}{2} Q_t h' + \frac{1}{2} Q_\infty h'$$

and substituting this expression in for $S(t)Q_\infty S^*(t)$ in the exponential

$$e^{-\frac{1}{2}<S(t)Q_\infty S^*(t)h', h'>} = e^{\frac{1}{2}<Q_t h', h'>} e^{-\frac{1}{2}<Q_\infty h', h'>}$$

gives

$$\hat{\mu}(S^*(t)h') e^{-\frac{1}{2}<Q_t h', h'>} = \hat{\mu}(h')$$

which is Condition (3.9). **QED**

The corollary is nothing but the classical computation of the (weighted) invariant measure for an Ornstein-Uhlenbeck process.

Theorem 3.1.3 *The stochastic process defined by equation (3.6) and the colored noise (3.7) is an SOC process. It has complex transients if the difference of some of the coefficients* $\alpha_1 - \frac{p}{q}\alpha_k,\ k \geq 2,\ p,q \in \mathbb{Z}^+$*, that determine the t scaling of V, is not a rational number.*

Proof: The proof of the five conditions in Definition 3.1.1 is similar to the proof of Lemma 3.1.1. We need to prove the condition in Definition 3.1.2. By the Equation (3.8)

$$\sum_{k=0,\ \alpha_k \neq 0}^{\infty} Q_t^k = \sum_{n=1} \sum_{k=0,\ \alpha_k \neq 0} \frac{(2\lambda_k)^{n-1} c_k}{\prod_{j=1}^{n} (j - 2\alpha_k)} t^{(n-2\alpha_k)}, \tag{3.10}$$

it is clear that some $Q_t^{k_1}$ will dominate initially with the t exponent $n_1 - 2\alpha_1$, where n_1 is a positive integer or zero. Later on during the initial transients, other Q_t^ks may dominate with a smaller exponent $n_2 - 2\alpha_2$, etc. If the difference $\alpha_1 - \frac{p}{q}\alpha_2$ is not a rational number, then these exponents are rationally independent. **QED**

Remark 3.1.1 In practice it may be impossible to check the conditions in Definition 3.1.2 or Definition 3.1.3, because any irrational number can be approximated arbitrarily closely by a rational one. Thus in real application we interpret these conditions to say that no low order rational dependence can be found, or one with *not very large* integers $p,q \in \mathbb{N}$.

Remark 3.1.2 We have presented a one-dimensional existence theory for the SPDEs in this section but all the statements apply and are similar in higher dimensions. The only difference is that in order for the stochastic processes solving the SPDEs to be continuous, the spatial coloring coefficients c_k, in Equations (3.3) and (3.7), must decay faster with k in higher dimensions; see Walsh [76]. Moreover, it turns out that it is the one-dimensional theory that applies to the fluvial landsurfaces discussed below although these surfaces are themselves two-dimensional.

The reasons are that there is a strong bias initially, introduced by the initial slope of the surface and the numerical scaling results, see [10], apply to one-dimensional cross-sections, perpendicular to the down-slope direction of the surface. Later on as the erosion process approaches more mature landscapes, there is an interplay between the initial channelization that is still active in the bottom of the valleys along the main rivers, and the adolescence and maturation processes that act on the slopes of the mountains, perpendicular to the (initial) down-slope direction. Thus the adolescence and maturation processes must also be gaged by a one-dimensional scaling in the direction perpendicular to the (initial) down-slope direction; see [10] and below.

Chapter 4

Fluvial Landsurfaces

Fluvial landsurfaces are described by two coupled nonlinear PDEs, see [10]. H denotes the height of the water surface and h denotes the water depth. This implies that $z = H - h$ is the height of the landsurfaces, but it is easier to describe the evolution in terms of the first two variables. We therefore focus our attention on the model

$$\eta^2 \frac{\partial h}{\partial t} = \nabla \cdot \left[\frac{\nabla H}{|\nabla H|} h^{\frac{5}{3}} |\nabla H|^{\frac{1}{2}} \right] + R, \tag{4.1}$$

$$\frac{\partial H}{\partial t} - \eta \frac{\partial h}{\partial t} = \nabla \cdot \left[\frac{\nabla H}{|\nabla H|} h^{\frac{5}{3}\gamma} |\nabla H|^{\frac{\gamma}{2}+\delta} \right] \tag{4.2}$$

in which we have adopted the scaling relation $[h]/[H] = [q_w]/[q_s] \equiv \eta$, η being a small parameter and R being the rainfall rate.

We use the same boundary and initial conditions as [71, 74] to model a linear ridge extending uniformly in the lateral (x)-direction and defined over a rectangular domain of length L and

width K,

$$D = \{(x,y) \in \mathbb{R}^2 | 0 \le x \le L,\ 0 \le y \le K\},$$

with initial conditions corresponding to a ridge of height cK uniform in the x-direction and with slope c in the y-direction,

$$\begin{aligned} h(x,y,0) &= d(y),\ d(y) = h_o,\ 0 \le y \le K - \varepsilon \\ &\qquad d(y) = h_o \frac{K-y}{\varepsilon},\ K - \varepsilon \le y \le K; \\ H(x,y,0) &= cy + d(y),\quad 0 \le y \le K, \end{aligned} \tag{4.3}$$

and boundary conditions

$$\begin{aligned} h(x,K,t) &= 0, \\ H(x,0,t) = &\quad h_0 \quad = h(x,0,t) \end{aligned} \tag{4.4}$$

corresponding to a water depth of zero at the top of the ridge and an absorbing body of water at the base of the ridge. While the water surface must be considered to be a free surface at the top of the ridge, it may be viewed as consisting of finitely many smooth curves that are solutions of a nonlinear ODE (the PDE restricted to the boundary). These curves are joined in a continuous, but not smooth, moving boundary (see, for example, Figure 4.2 that is borrowed from [10]). The upper boundary is characterized by the additional conditions

$$q_w = q_s = 0,$$

where

$$q_w = \frac{\nabla H}{|\nabla H|} h^{\frac{5}{3}} |\nabla H|^{\frac{1}{2}},\quad q_s = \frac{\nabla H}{|\nabla H|} h^{\frac{5}{3}\gamma} |\nabla H|^{\frac{\gamma}{2}+\delta}$$

are the water and sediment flux respectively, see [71], indicating the absence of any flux of water or sediment over this boundary. Since q_w and q_s are expressed as powers of h and ∇H in the constitutive relations, these conditions imply that the vanishing of the water depth dominates the blow-up of the gradient of H (in q_w and q_s) and that the normal derivative of H may become infinite at the upper boundary

$$n \cdot \nabla H(x,K,t) = \infty.$$

We will choose the values of the sediment transport parameters $\gamma = 2, \delta = 2$, which are realistic values for a range of landsurfaces. We note that there is no significant variation of our results in a whole neighborhood of such values of γ and δ. The boundary conditions on the lateral boundaries of the ridge at $x = 0$ and $x = L$ are taken to be periodic, modeling a linear ridge of infinite extent.

Water flowing down a uniform erodible sediment surface forms small channels that quickly cover the whole surface, see [71] and [10]. We will first examine what happens following this initial channelization process. In particular, we assume that our perturbed solutions take the form

$$h(x,y,t) = h_1(x,y,t) + v(x,y,t), \;\; H(x,y,t) = H_1(x,y,t) + u(x,y,t)$$

where $H_1(x,y,t)$ represents a convex[1] portion of an interfluvial ridge, see Figure 4.2 at 10% of the sediment eroded. The function $h_1(x,y,t)$ is the depth of water flow over this portion, and $v(x,y,t), u(x,y,t)$ are respectively the small perturbations to these quantities. The equations linearized about the convex profiles are

$$\eta^2 \frac{\partial v}{\partial t} = \nabla \cdot \left[\frac{5}{3} h_1^{\frac{2}{3}} \frac{\nabla H_1}{|\nabla H_1|^{1/2}} v \right] + \tag{4.5}$$

[1]Here and below the meaning of convex and concave is opposite to their mathematical definition in accordance with the use of these terms in geomorphology

$$\nabla \cdot \left[h_1^{\frac{5}{3}} \frac{\nabla u}{|\nabla H_1|^{1/2}} - \frac{1}{2} h_1^{\frac{5}{3}} (\nabla H_1 \cdot \nabla u) \frac{\nabla H_1}{|\nabla H_1|^{5/2}} \right],$$

$$\begin{aligned} \frac{\partial u}{\partial t} &= \nabla \cdot \left[\frac{h_1^{\frac{5}{3}}}{|\nabla H_1|^{1/2}} (\frac{1}{\eta} + h_1^{\frac{5}{3}} |\nabla H_1|^{5/2}) \nabla u \right] + \nabla \cdot \left[\frac{5}{3} h_1^{\frac{2}{3}} \frac{\nabla H_1}{|\nabla H_1|^{1/2}} (\frac{1}{\eta} + 2h_1^{\frac{2}{3}} |\nabla H_1|^{5/2}) v \right] \\ &+ \nabla \cdot \left[h_1^{\frac{5}{3}} (\frac{-1}{2\eta} + 2h_1^{\frac{5}{3}} |\nabla H_1|^{5/2}) (\nabla H_1 \cdot \nabla u) \frac{\nabla H_1}{|\nabla H_1|^{5/2}} \right], \end{aligned} \tag{4.6}$$

The first equation is a hyperbolic equation for v driven by ∇u. The second equation is a parabolic equation for u driven by v and ∇v.

Because water flows down the gradient of the surface $H_1(x,y,t)$, we may view the first equation as a hyperbolic PDE in one space dimension. Namely, if we let $\mathbf{u} = \frac{\nabla H_1}{|\nabla H_1|}$ denote the unit vector in the direction of the gradient of the water surface, we can write the first equation in the form

$$\eta^2 \frac{\partial v}{\partial t} = \frac{5}{3} h_1^{\frac{2}{3}} |\nabla H_1|^{1/2} \frac{\partial v}{\partial s} + g(x,y,t)v + f(x,y,t). \tag{4.7}$$

where the scalar s parametrize the direction of the gradient, $\frac{\partial v}{\partial s} = \mathbf{u} \cdot \nabla v$. This equation is analyzed in the Appendices in [10], where it is shown that *it develops shocks if the profiles about which we linearize are convex* or have knick-point singularities.

The original nonlinear system (4.1,4.2) can be completely analyzed in the direction of the maximal (negative) gradient of H because then it becomes one-dimensional. This is done in [78] and to some extent in [79]. It is shown that an initially linear profile develops a shock in the water flow, when a small perturbation is inserted at the top. This shock is a bore that propagates downstream; in the wake of the shock is another shock in the water surface, a hydraulic jump that digs up sediment. In the increased water volume between the stationary hydraulic jump and the traveling bore sediment is deposited. If this process is repeated in several storms it results

in a convex hillslope as in Figure 4.2 at 10% eroded.

The typical profile of the water surface is illustrated in Figure 4.1 borrowed from [78]. It shows a propagating bore in front and stationary hydraulic jump in the back; the origin is the top of the slope, with increased water height in between. The original height of the landsurface is $y = 0$. The upshot of all of this is that since the water is rather uniformly distributed over the

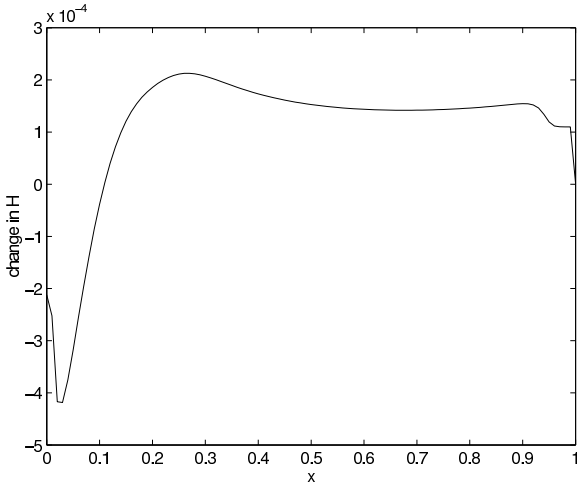

Figure 4.1: The profile of the water surface with a bore and a hydraulic jump

whole surface, up to the formation of H_1, the small white noise is magnified into *large colored noise*. Namely, the statistics of bores and hydraulic jumps are those of pinned Burger's shocks, see [50] and [66]. In this phase the surface is evolving rather rapidly and it seems appropriate to call this the *adolescence* of the surface. We will see below that the adolescence phase possesses its own characteristic scaling.

After the initial channelization some channels grow into river valleys separated by ridges and this landscape evolves through adolescence, see [71] and [10], toward a mature landscape that persists for a long time. The water flow down the slope of a mature landscape and the resulting scaling of the water (and land) surface is different from the scaling of channelization or the adolescence. To find and analyze this other scaling we linearize equations (4.1) and (4.2) about the separable solutions, see [71] and [65], representing the mature landscapes of valleys

and ridges [2]

$$H = H_2(x,y,t) + \varepsilon u(x,y,t), \;\; h = h_2(x,y.t) + \varepsilon v(x,y,t),$$

where $H_2 = H_o(x,y)T(t), \;\; h_2 = h_o(x,y)T^{-\frac{3}{10}}(t)$, are the separable solutions of the equations (4.1, 4.2). The form of the equations that we obtain for $u(x,y,t), \; v(x,y,t)$ by this linearizion process is the same as that characterizing the early period of channel emergence discussed above, namely (4.5) and (4.6), but with the terms $H_1(x,y,t), \;\; h_1(x,y,t)$ replaced by the separable solutions $H_2, \;\; h_2$.

Again, the first equation is a hyperbolic equation for v driven by ∇u and the second is a parabolic equation for u driven by v and ∇v. Since the first equation is really a hyperbolic PDE in one space dimension, exactly as in equation (4.7), we let the scalar s parametrize the direction of the gradient to obtain

$$\eta^2 \frac{\partial v}{\partial t} \;=\; \frac{5}{3} h_2^{\frac{5}{3}} |\nabla H_2|^{1/2} \frac{\partial v}{\partial s} \;+\; g(x,y,t)v \;+\; f(u,t). \tag{4.8}$$

A straight-forward analysis of this equation, presented in an Appendix in [10], shows that its solutions develop shocks, for separable surfaces with (slope) singularities, since concave slopes with knick-points are the dominant feature of the mature separable landscape, as illustrated in Figure 4.2, at 60% of the sediment eroded. More importantly for the mature surfaces the nonlinear water equations (4.1) have turbulent solutions, see [9]. This turbulent water flow feeds sediment divergences and generates colored noise in the linearized equations, see [10].

However, analogous to the adolescent phase, the linearized sediment equation is simply a reflection of what happens in the full nonlinear equations (4.2). These nonlinear PDEs can be analyzed, as above, in the direction of the maximal gradient of the separable surfaces and this

[2] As in our previous analysis, we employ sediment transport parameter values $\gamma = \delta = 2$, noting that similar results hold for parameter values in a neighborhood of these.

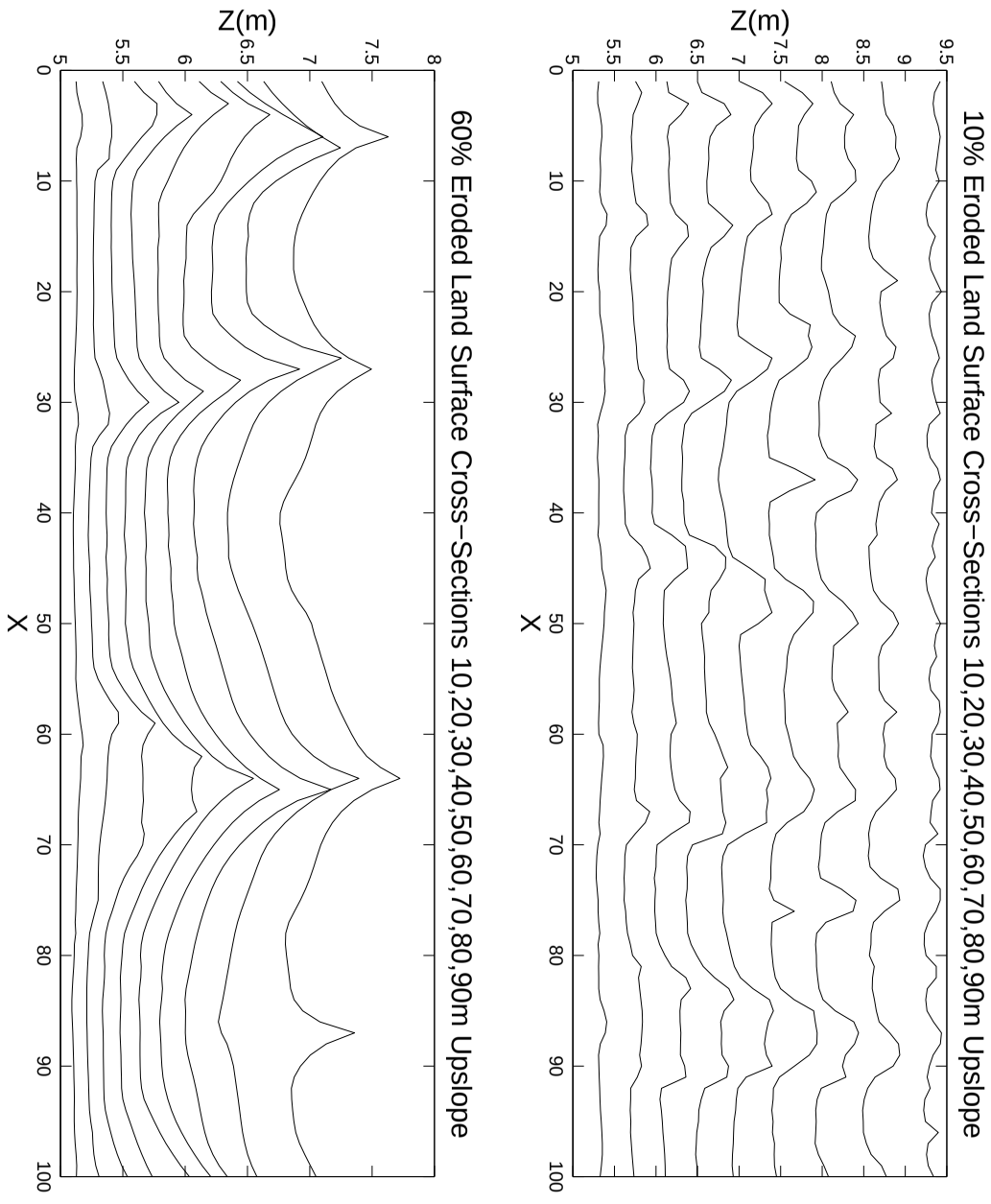

Figure 4.2: Transverse Sections at 10m separation on the Eroding Ridges at 10% and 60% Eroded

is done in [78] and [79]. Now the noise is also colored and this coloring process is analyzed in great detail in [78]. Once the convexity, created between the bore and the hydraulic jump discussed above, meets the lower boundary a small concavity is created. This produces a shock in the gradient of the sediment flow; its profile in the riverbed is called a knick-point. The shock travels upstream; once it get all the way to the top of the hillslope a concave profile has been carved out; see Figure 4.2 at 60% eroded. The arrival of the knick-point at the upper ridge completes the evolution of the tranport limited river profile but a similar evolution is also taking place on all the hillsides of all mature landsurfaces. Bores and hydrolic jumps are widely observed and it is well known that knick-points (rapids) travel upstream in time.

The coloring process described in [78] proceeds as follows. A small perturbation at the lower boundary is turned into small cavity in the hillslope which then travels upstream. In Figure 4.3 borrowed from [78] we see the slope $-H_x$ of the water surface as the knick-point approaches the upper boundary. Now the small perturbation gets magnified into a singularity

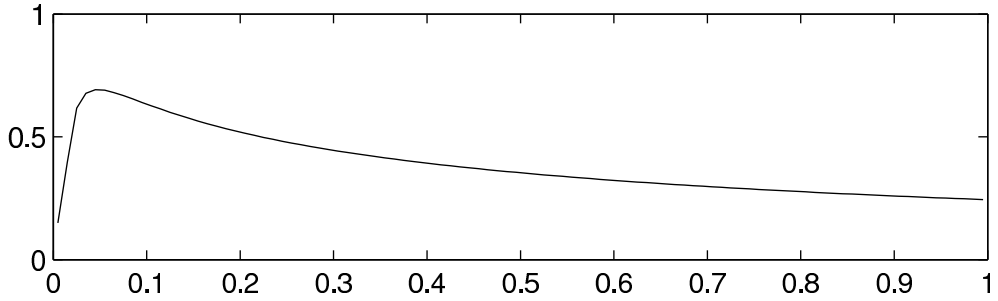

Figure 4.3: The slope of the water surface as a function of the downslope direction, showing a knick-point approaching the upper boundary, at $x = 0$.

in the derivative of the slope, that is highly colored in space and represented by a Hölder continuous function; see [78] for more details. Moreover, since there is very little water on top of the mature ridges, the distribution of the shocks is no longer uniform in space. We conclude that the equations linearized about the separable surfaces are driven by large noise which is highly colored in space and polynomially colored in time due to the decay of the separable sur-

faces in time. This flow over a knick-point seems to be a primary example of one-dimensional turbulence, see [9] for further analysis.

Chapter 5

The Channelization, Adolescence and Maturation Processes

Channelization and Adolescence

In this section we will discuss the three stochastic processes determined by the equations (4.1) and (4.2) linearized about the initial channelizing surface (h_0, H_0), and the convex (h_1, H_1) and concave (h_2, H_2) surfaces respectively.

Consider the linearized equation describing the Channelization Process

$$
\begin{aligned}
\frac{\partial u}{\partial t} &= \nabla \cdot \left[\frac{h_0^{\frac{5}{3}}}{|\nabla H_0|^{1/2}} \left(\frac{1}{\eta} + h_0^{\frac{5}{3}} |\nabla H_0|^{5/2} \right) \nabla u \right] \\
&+ \nabla \cdot \left[h_0^{\frac{5}{3}} \left(\frac{-1}{2\eta} + 2h_0^{\frac{5}{3}} |\nabla H_0|^{5/2} \right) (\nabla H_0 \cdot \nabla u) \frac{\nabla H_0}{|\nabla H_0|^{5/2}} \right] \\
&+ \nabla \cdot \left[\frac{5}{3} h_0^{\frac{2}{3}} \frac{\nabla H_0}{|\nabla H_0|^{1/2}} \left(\frac{1}{\eta} + 2h_0^{\frac{2}{3}} |\nabla H_0|^{5/2} \right) v \right],
\end{aligned}
\tag{5.1}
$$

Initially the channels are very small, and the slope $|\nabla H_0|$ is going to be very small. We will make the assumption that $\frac{h_0^{\frac{5}{3}}}{|\nabla H_0|^{1/2}} <$ constant, except on a set of measure zero. Then ignoring terms that are small the equation (5.1) becomes

$$\frac{\partial u}{\partial t} = a\Delta u + c\frac{\partial v}{\partial x} \tag{5.2}$$

where a and c are constants. The reason for this is that the ratio $\frac{h_0^{\frac{5}{3}}}{|\nabla H_0|^{1/2}}$ is approximately a constant and all the terms multiplied by $|\nabla H_0|$ are small and can be ignored. Thus the equation (5.1) reduces to the equation considered in Section 3, if ∇v is white noise. To verify this we solve the equation

$$\eta\frac{\partial v}{\partial t} = b\frac{\partial v}{\partial s} + \sum_{k=0}^{\infty} dB_t^k e_k(x) \tag{5.3}$$

obtained from Equation (4.7), with H_1 replaced by H_0, by ignoring terms that are small and adding the noise in the initial water flow. We have also canceled one power of η by a small term ($|\nabla H_0|$) on the right hand side of the equation and b is a constant. Now setting $\eta = 0$ it becomes clear that $\frac{\partial v}{\partial s} = \mathbf{u}\cdot\nabla v$ is white noise.

Next we solve the SPDE

$$dU = \Delta U dt + dW \tag{5.4}$$

where

$$W = \sum_{k=0}^{\infty} B_t^k e_k(x) \tag{5.5}$$

is our model for the (white) noise term in equation (5.1) where the e_ks are the one-dimensional eigenfunctions of $-\Delta$ and B_t^ks are independent and Brownian. Then an analogous proof to that of Theorem 3.0.1, recalling that the initial water surface is $H_0(0)$, proves the following theorems.

Theorem 5.0.4 *Assume that the last term in equation (5.1) can be modeled by white noise, then*

the Channelization process u defined by equation (5.1) is a Edward-Wilkinson process and

$$H = H_0(0,x,y_o) + \sum_{k=0}^{\infty} A_t^t e_k(x)$$

constitutes Brownian motion of the channelizing surface, for every fixed y_o, where the

$$A_t^k = e^{-\lambda_k t} A_0^k + c_k^{\frac{1}{2}} \int_0^t e^{-\lambda_k (t-s)} dB_s^k,$$

are independent Orstein-Uhlenbeck processes.

Theorem 5.0.5 *The Channelization Process possesses a transient growth state where the width function, of the slope ∇H, grows with a temporal roughness exponent*[1] *of $\frac{1}{4}$*

$$V((x,y),(z,y),t) \leq t^{\frac{1}{4}}.$$

The process eventually gets into a statistically stationary state, where the width function has a spatial roughness coefficient of $\frac{1}{2}$

$$V((x,y),(z,y),t) \leq C|z-x|^{\frac{1}{2}}.$$

There exists an invariant measure residing on the whole space.

Corollary 5.0.3 *The Channelization Process is not an SOC process.*

Proof: The proof is the same as the proof of Theorem 3.0.2 and Corollary 3.1.1 **QED**

The numerical simulations in [10] are done by considering a lag variable $z-x$ in the x direction for a fixed y (upslope direction). χ is called a scaling exponent if V scales with the exponent

[1] The notation $(x,y),(z,y)$ indicates that the lag variable $z-x$ is in the direction of the x axis.

χ over a range of upslope values y all the way from the lower to the upper boundary. The scaling brakes down close to the boundaries because of their influence. The theorem proves the numerical observations in [10], see also [11]. Because of the bias caused by the initial slope $H_o = cy + d(y)$, ∇H, but not H, scales initially and the bias causes the scaling exponent to appear as $\chi/2$, see the appendix in [10] for the details. Moreover, initially, the water depth h scales as Brownian motion, in the computations, lending support to our modeling of the noise (5.5).

We consider the equations (4.1) and (4.2) linearized about the the convex surface (h_1, H_1),

$$
\begin{aligned}
\frac{\partial u}{\partial t} &= \nabla\cdot\left[\frac{h_1^{\frac{5}{3}}}{|\nabla H_1|^{1/2}}(\frac{1}{\eta}+h_1^{\frac{5}{3}}|\nabla H_1|^{5/2})\nabla u\right] \\
&+ \nabla\cdot\left[h_1^{\frac{5}{3}}(\frac{-1}{2\eta}+2h_1^{\frac{5}{3}}|\nabla H_1|^{5/2})(\nabla H_1\cdot\nabla u)\frac{\nabla H_1}{|\nabla H_1|^{5/2}}\right] \\
&+ \nabla\cdot\left[\frac{5}{3}h_1^{\frac{2}{3}}\frac{\nabla H_1}{|\nabla H_1|^{1/2}}(\frac{1}{\eta}+2h_1^{\frac{2}{3}}|\nabla H_1|^{5/2})v\right],
\end{aligned}
\tag{5.6}
$$

We have linearized the equations (4.1) and (4.2) about a fixed profile $H(x,y,t_0) = H_1(x,y)$, $h(x,y,t_0) = h_1(x,y)$. The variable v describes perturbations of the water depth; it solves a hyperbolic equation and will develop shocks but more importantly the solutions H_1 (and h_1) contain the bores and the hydraulic jumps as described in the previous section. Thus the last two terms in the equation (5.1) contain *large colored noise*, where the color $\chi = 2/3$ is similar to that of shock solutions of Burger's equation with multiplicative noise and a pinning force, see [78] and Parisi [50] and Sneppen [66].

Lemma 5.0.5 *If* $0 < |\frac{h_1^{\frac{5}{3}}}{|\nabla H_1|^{1/2}}|_\infty < \infty$ *in* Ω *except on a set of measure zero, then the operator*

$$\begin{aligned} Au &= \nabla \cdot \left[\frac{h_1^{\frac{5}{3}}}{|\nabla H_1|^{1/2}} (\frac{1}{\eta} + h_1^{\frac{5}{3}} |\nabla H_1|^{5/2}) \nabla u \right] \\ &+ \nabla \cdot \left[h_1^{\frac{5}{3}} (\frac{-1}{2\eta} + 2h_1^{\frac{5}{3}} |\nabla H_1|^{5/2}) (\nabla H_1 \cdot \nabla u) \frac{\nabla H_1}{|\nabla H_1|^{5/2}} \right] \end{aligned}$$

is dissipative and generates a continuous contraction semi-group.

Proof: The operator A is clearly symmetric on the Hilbert space $L^2(\Omega)$ with boundary conditions that vanish on half of $\partial\Omega$ and are periodic on the other half of $\partial\Omega$, see the equations (4.1) and (4.2). A is defined on the subset of smooth functions $C^\infty(\Omega) \subset L^2(\Omega)$, so A is a closed operator. To show that A is dissipative if suffices to show that

$$< u, Au > \leq 0,$$

for all $u \in L^2(\Omega)$, where $<,>$ denotes the inner product in $L^2(\Omega)$, but

$$\begin{aligned} < u, Au > &= < u, \nabla \cdot \left[\frac{h_1^{\frac{5}{3}}}{|\nabla H_1|^{1/2}} (\frac{1}{\eta} + h_1^{\frac{5}{3}} |\nabla H_1|^{5/2}) \nabla u \right] > \\ &+ < u, \nabla \cdot \left[h_1^{\frac{5}{3}} (\frac{-1}{2\eta} + 2h_1^{\frac{5}{3}} |\nabla H_1|^{5/2}) (\nabla H_1 \cdot \nabla u) \frac{\nabla H_1}{|\nabla H_1|^{5/2}} \right] >= \\ -\| (\frac{h_1^{\frac{5}{3}}}{|\nabla H_1|^{1/2}} (\frac{1}{\eta} &+ h_1^{\frac{5}{3}} |\nabla H_1|^{5/2}) |\nabla u|^2 + h_1^{\frac{5}{3}} (\frac{-1}{2\eta} + 2h_1^{\frac{5}{3}} |\nabla H_1|^{5/2}) \frac{1}{|\nabla H_1|^{5/2}} (\nabla H_1 \cdot \nabla u)^2)^{1/2} \| \\ &\leq -\| (\frac{h_1^{\frac{5}{3}}}{|\nabla H_1|^{1/2}} (\frac{1}{2\eta} h_1^{\frac{5}{3}} + 3|\nabla H_1|^{5/2}) |\nabla u|^2)^{1/2} \| \end{aligned}$$

by Schwartz's inequality applied to the vector product $(\nabla H_1 \cdot \nabla u)$, where $\|\cdot\|$ denotes the L^2

norm. Now since the last expression is negative, we conclude that

$$< u, Au > \leq 0.$$

Now it is easy to show that 1 lies in the resolvent set of A and this implies that A generates a C^0 semi-group, see Yosida [81], page 250. **QED**

The operator $-A$ is in fact essentially self-adjoint on $L^2(\Omega)$ with the hypothesis in Lemma 5.0.5 and has a sequence of eigenvalues $\lambda_k^{(2)} \to \infty$ and associated eigenfunctions $e_k(x,y)$.

We now solve the SPDE

$$dU = AUdt + dW \tag{5.7}$$

where

$$W = \sum_{k=0}^{\infty} c_k B_t^k e_k(x) \tag{5.8}$$

where the c_k have the spatial coloring $\chi = 2/3$ of the the KPZ (Burger's) equation with multiplicative noise and pinning force, see Parisi [50] and Sneppen [66].

Theorem 5.0.6 *Assume that the equation (5.6) is driven by the noise (5.8). Then the adolescent surfaces are described a stochastic Adolescence Process. The Adolescence Process possesses a transient growth state where width function, of the slope ∇H, grows with a temporal roughness exponent*[2] *of* $\frac{1}{3}$

$$V((x,y),(z,y),t) \leq t^{\frac{2}{3}}.$$

The process eventually gets into a statistically stationary state, where the width function has a spatial roughness coefficient of $\frac{2}{3}$

$$V((x,y),(z,y),t) \leq C|z-x|^{\frac{2}{3}}.$$

[2]The notation $(x,y),(z,y)$ indicates that the lag variable $z-x$ is in the direction of the x axis.

There exists an invariant measure residing on the whole space.

Corollary 5.0.4 *The Adolescence Process is an SOC process.*

Proof: The proof is the same as the proof of Lemma 3.1.1, with $\alpha_k = 0,\ 0 \leq k < \infty$. This restricts the dynamical exponent to be $z = 1$, corresponding to turbulent solutions of Burger's equation. The existence of a colored invariant measure follows from Corollary 3.1.2. **QED**

We will now explain why the one-dimensional examples in Sections 3-3.1 apply to the two-dimensional linearized equations in this Section. The reason is that both the evolution of the convex and the concave profiles in Figure 4.2 takes place in the direction of the maximal gradient of the water surface $|\nabla H|$ and can be restricted to an evolution with a one-dimensional spatial variable. This direction is of course never a straight line but it is mostly directed in the x direction. In the y (upslope) direction the initial surface dominates and gives a bias to the numerically computed scaling. Thus the scaling laws in [10] are obtained by cross-sections of the surfaces (convex and concave) in the x directions at fixed values of y. Statistically this is identical to the information gained by taking cross-sections along the directions of $\max|\nabla H|$; see [10] for more information on this issue.

The operator $-A$ has the same properties as above when restricted to one dimensional cross-sections. Namely, $-A$ is essentially self-adjoint on $L^2([0,L])$ with periodic boundary conditions and has a sequence of eigenvalues $\lambda_k^{(1)} \to \infty$ and associated eigenfunctions $e_k(x)$.

Maturation

We now linearized the equations (4.1) and (4.2) about a separable solution $H_2 = H_o(x,y)T(t)$, $h_2 = h_o(x,y)T^{-\frac{3}{10}}(t)$, describing a mature decaying landscape, see [71, 74, 10]. The resulting

equations are

$$\begin{aligned}\frac{\partial u}{\partial t} &= \nabla\cdot\left[\frac{h_o^{\frac{5}{3}}}{|\nabla H_o|^{1/2}}(\frac{T^{-1}}{\eta}+h_o^{\frac{5}{3}}|\nabla H_o|^{5/2}T)\nabla u\right]\\ &+ \nabla\cdot\left[h_o^{\frac{5}{3}}(\frac{-T^{-1}}{2\eta}+2h_o^{\frac{5}{3}}|\nabla H_o|^{5/2}T)(\nabla H_o\cdot\nabla u)\frac{\nabla H_o}{|\nabla H_o|^{5/2}}\right]\\ &+ \nabla\cdot\left[\frac{5}{3}h_o^{\frac{2}{3}}\frac{\nabla H_o}{|\nabla H_o|^{1/2}}(\frac{T^{3/5}}{\eta}+2h_o^{\frac{2}{3}}|\nabla H_o|^{5/2}T^{2\frac{9}{10}})v\right]\end{aligned} \tag{5.9}$$

and a hyperbolic equation for the water v depth as described in the previous section. The water depth can develop shock that are sources of noise, however in distinction to equation (5.1) this noise is highly colored in space due to the fact that the water depth goes to zero on top of the separable ridges, see [10], and the solutions H_o (and h_o) contain the colored knick-point shocks, described in previous section. In addition the noise term involving ∇v and v is colored in time due to the factors $T^{3/5}$, T and $T^{2\frac{9}{10}}$. We conclude that Equation (5.9) is driven by *large noise that is highly colored both in space and time.* The remaining T factor T^{-1} is removed in the following manner.

It is shown in [71] that the time decay T satisfies the ODE,

$$\frac{\partial T}{\partial t} = -aT^2$$

where $-a = \frac{F_o}{V_o}$ is the ratio of the sediment flux F_o to the volume $V_o = \int_\Omega H_o(x,y)dxdy$. This ODE is easily solved to give

$$T(t) = \frac{1}{(1+at)}$$

assuming that $T(0) = 1$. Substituting this expression in for T in the equation (5.9) and making

the change of variables $s = \frac{(1+at)^2}{2a}$ give the equation

$$\begin{aligned}
\frac{\partial u}{\partial s} &= \nabla \cdot \left[\frac{h_o^{\frac{5}{3}}}{|\nabla H_o|^{1/2}} (\frac{1}{\eta} + h_o^{\frac{5}{3}} |\nabla H_o|^{5/2} \frac{1}{2as}) \nabla u \right] \\
&+ \nabla \cdot \left[h_o^{\frac{5}{3}} (\frac{-1}{2\eta} + 2h_o^{\frac{5}{3}} |\nabla H_o|^{5/2} \frac{1}{2as}) (\nabla H_o \cdot \nabla u) \frac{\nabla H_o}{|\nabla H_o|^{5/2}} \right] \\
&+ \nabla \cdot \left[\frac{5}{3} h_o^{\frac{2}{3}} \frac{\nabla H_o}{|\nabla H_o|^{1/2}} (\frac{1}{(2a)^{4/5} s^{4/5}} + 2h_o^{\frac{2}{3}} \frac{|\nabla H_o|^{5/2}}{(2a)^{1\frac{19}{20}} s^{1\frac{19}{20}}} v \right] \qquad (5.10)
\end{aligned}$$

This equation is also driven by large noise, in the last two terms, colored by a quenched (by the absence of water on top of mountains) knick-point noise in space and polynomially colored in the time s.

Lemma 5.0.6 *If* $0 < |\frac{h_1^{\frac{5}{3}}}{|\nabla H_1|^{1/2}}|_\infty < \infty$ *in* Ω*, except on a set of measure zero, the operator*

$$A_o u = \nabla \cdot \left[\frac{h_o^{\frac{5}{3}}}{|\nabla H_o|^{1/2}} \frac{1}{\eta} \nabla u \right] + \nabla \cdot \left[h_o^{\frac{5}{3}} (\frac{-1}{2\eta}) (\nabla H_o \cdot \nabla u) \frac{\nabla H_o}{|\nabla H_o|^{5/2}} \right]$$

is dissipative and generates a continuous contraction semi-group whereas the operator

$$\begin{aligned}
A(s)u &= \nabla \cdot \left[\frac{h_o^{\frac{5}{3}}}{|\nabla H_o|^{1/2}} (\frac{1}{\eta} + h_o^{\frac{5}{3}} |\nabla H_o|^{5/2} \frac{1}{2cs}) \nabla u \right] \\
&+ \nabla \cdot \left[h_o^{\frac{5}{3}} (\frac{-1}{2\eta} + 2h_o^{\frac{5}{3}} |\nabla H_o|^{5/2} \frac{1}{2as}) (\nabla H_o \cdot \nabla u) \frac{\nabla H_o}{|\nabla H_o|^{5/2}} \right]
\end{aligned}$$

generates a solution operator $S(s, s_o)$ *for the equation (5.10), for* $1/\eta$ *large.*

Proof: The proof of the dissipativeness of A is the same as in Lemma 5.0.5 but simpler. For

$1/\eta$ large the quadratic form $< u, Au >$ bounds the form

$$< \nabla u, (h_o^{\frac{5}{3}} |\nabla H_o|^{5/2} \frac{1}{2cs} + 2h_o^{\frac{5}{3}} |\nabla H_o|^{5/2} \frac{1}{2as} (\nabla H_o \cdot \nabla u) \frac{\nabla H_o}{|\nabla H_o|^{5/2}}) \nabla u >$$

uniformly in s. This implies that the form $< u, A(s)u >$ generates a solution operator; see Kato [39]. **QED**

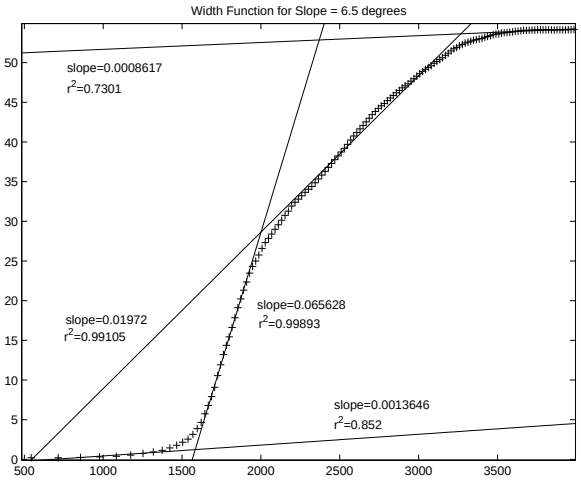

Figure 5.1: The scaling exponents of the variogram are shown as a function of time, for an initial surface with a slope of 6.5 degrees, on a log-log plot. The temporal evolution shows four different exponents (slopes), along with their regression coefficients, and a statistically stationary state (with slope zero) is emerging, furthest to the right.

The operator $-A_o$ is also essentially self-adjoint on $L^2(\Omega)$ with the hypothesis in Lemma 5.0.6 and once we restrict it to a one-dimensional cross-section as discussed above, it retains these properties on $L^2([0,L])$ and has a sequence of eigenvalues $\lambda_k \to \infty$ and associated eigenfunctions $e_k(x)$.

We now write the equation (5.9) restricted to a one-dimensional cross-section as a SPDE,

(5.11) $$dU = A_o U ds + dW_m$$

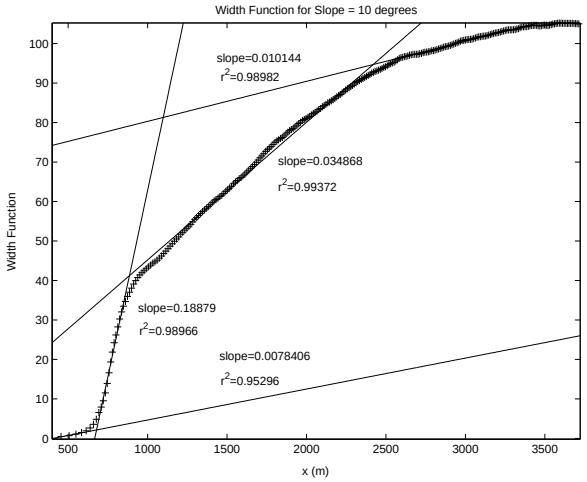

Figure 5.2: The scaling exponents of the variogram are shown as a function of time, for an initial surface with a slope of 10 degrees, on a log-log plot. The temporal evolution shows four different exponents (slopes), along with their regression coefficients, and a statistically stationary state (with slope zero) is emerging, furthest to the right.

where the noise

$$W_m = \sum_{k=0}^{\infty} \frac{c_k}{s^{\alpha_k}} B_s^k e_k(x)$$

is colored both in space (the c_ks) and time (the $s^{-\alpha_k}$s) and some (infinitely many) of the α_k are zero. The B_t^k are independent Brownian motions and we have ignored the deterministic part of the operator $A(s)$,

$$A(s) - A_o = \left[\frac{h_o^{\frac{5}{3}}}{|\nabla H_o|^{1/2}} (h_o^{\frac{5}{3}} |\nabla H_o|^{5/2} \frac{1}{2cs}) \nabla u \right].$$

If η is small this part is going to be very small compared to $1/\eta$ and can be added by regular perturbation theory. The same proof as that of Theorem 3.1.1 gives the following theorem.

Theorem 5.0.7 *Assume that the noise for mature landscapes has the color*

$$W = \sum_{k=0,\ \alpha_k \neq 0}^{\infty} \frac{c_k}{s^{\alpha_k}} B_s^k e_k(x) + \sum_{k=0,\ \alpha_k = 0}^{\infty} c_k B_s^k e_k(x), \tag{5.12}$$

then the mature landscapes are described by a stochastic Maturation Process

$$H(x,y_o,t) = \frac{H_o(x,y_o)}{(1+at)} + \sum_{k=0}^{\infty} A^k_{\frac{(1+at)^2}{2a}} e_k(x).$$

where the

$$A^k_{\frac{(1+at)^2}{2a}} = e^{-\lambda_k \frac{(1+at)^2}{2a}} A^k_0 + c_k^{\frac{1}{2}} \int_0^{\frac{(1+at)^2}{2a}} e^{-\lambda_k (\frac{(1+at)^2}{2a} - s)} s^{-\alpha_k} dB^k_s,$$

are independent. For k such that $\alpha_k = 0$, the $A^k_{\frac{(1+at)^2}{2a}}$s are Ornstein-Uhlenbeck processes.

Theorem 5.0.8 *Suppose that*

$$min_{n,k}(\frac{n}{2} - \alpha_k)_+ = \frac{1}{10},$$

i.e. $\alpha_2 = 1\frac{19}{20}$ *and that*

$$\sum_{k=0,\alpha_k=0} \frac{c_k}{\lambda_k^{1-\chi}} < \infty,$$

for $\chi \leq 0.75$*, then the Maturation Process possesses a transient growth state where its width function, of the water surface H, grows with a temporal roughness exponent*[3] *of* 0.10

$$V((x,y),(z,y),t) \leq t^{0.10},$$

and the process eventually gets into a statistically stationary state, where the width function has a spatial roughness coefficient of 0.75

$$V((x,y),(z,y),t) \leq C|z-x|^{0.75}.$$

Proof: We apply Lemma 3.1.4 to the Equation (5.11), that models Equation (5.10), with the noise (5.12). Then the Theorem follows from Theorem 3.1.1 observing that if V^2 scales by $s^{\frac{1}{10}}$ then $(s^{\frac{1}{10}})^{1/2} = s^{\frac{1}{20}} = (c(t_0+t)^{\frac{1}{10}}) \approx Ct^{0.10}$ for t_0 small. This means that V scales as $t^{0.10}$.

[3]The notation $(x,y),(z,y)$ indicates that the lag variable $z-x$ is in the direction of the x axis.

QED

Theorem 5.0.9 *The Maturation Process projects, as t becomes large, onto a subspace,* $H' = \{x' = \sum x_k e_k | \alpha_k = 0\}$, *of the phase space* $L^2([0,L])$, *where there exists an invariant measure.*

Proof: This is a direct consequence of Theorem 3.1.2. **QED**

Corollary 5.0.5 *The Maturation Process is an SOC process.*

Proof: By Corollary 3.1.2 the invariant measure is a weighted Gaussian. Thus the process satisfies Conditions 1-5 of Definition 3.1.1. **QED**

Remark 5.0.3 The verification of the fact that the Maturation Process has complex transients is so far numerical. There are two exponents in Equation (5.10), $4-3\frac{9}{10} = 0.1$ and $2-1\frac{3}{5} = 0.4$. In the roughening of the surface, the latter exponent is dominated by the first (which is smaller) and does not show up. Numerically, two smaller coefficients dominate later during the transients, see Figure 1.1 and Figures 5.1 and 5.2. Thus numerically the Maturation Process satisfies Definition 3.1.2 and this is presumably due to the small terms we omitted, that give corrections with t exponents smaller than 0.1.

Numerically there is a trade off between the length of the computations and the instabilities that set in with larger slope. In Figure 1.1 we strike a balance with slope 8.5 degrees and get an initial coefficient of 0.127 that persists. This is in rough agreement with the theory. In Figure 5.1, with a slope of 6.5 degrees, we are not quit far enough into the maturation phase although the computing time is already extremely long and get a slope of 0.066. In Figure 5.2 the slope of 10 degrees is rather unstable and we get the slope 0.189.

Remark 5.0.4 The upper-cutoff for the spatial scaling of the landsurfaces is not the system size L but the half-width of the valleys ℓ. Hack's law implies that for young channelizing landsurfaces, 10% eroded,

$$0.1cK \sim \ell^{1/2}, \ \ell \sim 0.01(cK)^2$$

where cK is the height of the mountain range (K is the width in the y direction and c the slope), whereas

$$0.5cK \sim \ell^{3/4}, \ \ell \sim 0.40(cK)^{4/3}$$

for a mature landsurface, 50% eroded. This means that mature valleys typically (unless cK is large) are wider than young ones and the number N of valleys is,

$$N \sim \frac{L}{0.02(cK)^2},$$

for young surfaces, L being the length (in the x direction) of the mountain range, whereas

$$N \sim \frac{L}{0.80(cK)^{4/3}},$$

for the mature landsurfaces. This says that mature surfaces typically (unless cK is large) have fewer valleys than the young surfaces.

Discussion: We showed that the three processes Channelization, Adolescence and Maturation are driven by large noise terms, white for the first and colored both in space and time for the latter two processes. These noise terms are created by shocks, bores and hydraulic jumps in the second case and turbulent flow and knick-points in the second case, see [78] and [9]. In addition the noise in the Maturation case is colored in time by the fact that the separable surfaces have a distinct polynomial decay in time. This analysis allows us to associate these three processes with solution of one-dimensional linear SPDEs driven by the three different types of noise above.

It would be more desirable to solve the nonlinear PDEs directly and read of all the above information. This may be doable in the case of the Channelization Process where channelization is working on the whole two-dimensional surface. Numerically, the bias of the initial surface is

removed by considering ∇H that scales over the whole surface. But this is more complicated in the adolescence and maturation cases where the Adolescence and Maturation Processes are working on the slopes of the separable mountains but the Channelization Process still works on the bottom of the valleys. In fact for the mature landscape the scaling properties of the river basin, such as Hack's law, may be understood by putting two of those processes together; see [10]. It may be that one-dimensional theory analogous to the numerical results in [78] is the ultimate result for the Adolescence and Maturation Processes. In any case it remains to show that the full transport limited landsurface evolution is a Markovian Stochastic Process determined by the solutions of the full nonlinear PDEs, entraining large noise; and that these solutions reduce to the three processes above, close to the initial channelizing surface $H_0(x,y,t)$, the convex surfaces $H_1(x,y,t)$ and separable surfaces $H_2 = H_o(x,y)T(t)$ respectively. This is what the numerical and analytical results indicate.

5.1 Applications and Limitations of the Theory

The theory presented here captures well the evolution of landsurfaces for transport-limited situations, such as one would typically find in desert environments. The scaling exponents are in good agreement with the numerical simulations [10] both for the channelization process, that channelizes the initial surface, the adolescence process that evolves it from a convex to a concave surface, and the maturation process that does the ultimate sculpting of the mature surface. The agreement is good for the scaling exponents in the stationary states; see [10], and reasonably good during the initial transients of the maturation phase, as shown in Figures 5.1, 1.1 and 5.2[4]. In these figures the scaling exponent of the initial transient into the maturation phase β_2 ranges from 0.066 for slope 6.5, 0.127 for slope 8.5, to 0.189 for slope 10. The time-scale for these transients is geological time and they take a very long time to compute and are very

[4]These computations were done by Kirsten Meeker using an analysis program developed by Russell Schwab.

sensitive to the value of the slope. However, the average is reasonably close to the theoretical value of 0.1 for β_2 in Theorem 5.0.8.

The picture is obviously more complicated for real landsurfaces. Erosion takes place on a surface that may already have a complicated form and since the transients take place on a geological time-scale it is not clear how the temporal scaling exponents can be measured. The spatial exponents can on the other hand be measured from DEM (digital elevation model) data and in [10] the numerically computed exponents were compared to exponents from a DEM [77], with satellite data from Ethiopia, Somalia and Saudi-Arabia. The exponents measured in this DEM fall in the range spanned by the spatial exponents of the channelization, the adolescence and the maturation phases.

The magnification of the noise by the nonlinearities (the initial surface is seeded by tiny random perturbations) is understood, see [10], [78] and [79]. The reason is that both the water and sediment flow down the gradient of the water surface and the magnification can be understood as shock formation in one dimension. This was pointed out in [10], and worked out in [78] , [79]. The details, presented in [78] , confirm the prediction for the mechanism of the formation of transport-limited surfaces in [71]. The shocks that carve out the concave mature slopes are traveling knick-points. Thus the theory is completed by inserting the bores and hydraulic jumps and the traveling knick-points into the noise in the adolescence phase. In the maturation phase the color of the noise stems form turbulent water flow, see [9], including flow over these same knick points (rapids) as the surfaces mature. In addition to these results one would like to prove the existence of an invariant measure for the full nonlinear PDEs (4.1) and 4.2) with these noise inputs. For now, however, this is beyond our mathematical reach.

5.1.1 The SOC Theory

The theory presented is essentially the mathematical version of the theory of Self-organized-critical systems in the physics literature. The systems have two phases a transient and a stationary phase characterized by the scaling of the variogram. The idea of an SOC attractor is replaced by an infinite-dimensional subspace that attracts the dynamics. On this subspace there exists an invariant measure that contains all the information about the stationary state. The system is seen to temporarily self-organize during the transients in a rather trivial way. Either it approaches the stationary state in the subspace where the stationary state lives or the motion is in the orthogonal complement of this subspace and is eventually projected out. However, the structure or scaling of the stationary state is gradually formed during the transients. It is explicitly expressed in how the different directions are weighted (colored) in the invariant measure. This is how the stationary state is *self-organized* during the transients.

The mathematical model clarifies the role of instabilities and nonlinearities. The instabilities make small perturbation grow and these dynamics are then colored by the nonlinearities. Whether and how this coloring takes place plays an important role in the structure of the stationary state.[5] The color produces long range spatial correlations in the stationary phase and long range temporal correlations in the transient phase. Thus it is clear by examining the conditions in Example 3.1.1 and 3.1.4, that any temporal exponents $0 < \beta \leq 1/4$ is possible in one dimension and any spatial exponent $1/2 \leq \chi < 1$. The long range correlations are given by $0 < \beta < 1/4$ and $1/2 < \chi < 1$ respectively, if $z = 2$. The Edward-Wilkinson process (Channelization and Brownian motion) sits at the boundary of these intervals, with $\beta = 1/4$ and $\chi = 1/2$. The Adolescence Process is short-range for t, $\beta = 2/3$, and long-range for x, $\chi = 2/3$, because in this case $z \neq 2$, in fact $z = 1$. The Maturation Process is long-range with $\chi = 3/4$ and here again $z = 2$.

[5] One might therefore be tempted to interpret SOC to mean ”systems of color”.

The transport-limited erosion model gives us three processes. One, the channelization where the white noise in the environment is magnified but not colored, resulting in channelization that is an Edward-Wilkinson process driven by white noise. The other two processes are driven by highly colored noise because of the non-uniform distribution of water over the adolescent and mature surface and the coloring of the system by bores and hydraulic shocks and knick-points in the adolescent phase. The noise on the mature surfaces is created by turbulent water flow over knick point and these concave mature surfaces. The Adolescent and Mature Processes are SOC processes with long range correlations. In addition the Maturation Process possesses complex transients that scale with several temporal exponents.

The above theory is not restricted to linear equations, linearizing about known profiles as in the landsurface case, the modification for nonlinear SPDEs is straightforward, see [51]. Suppose we start with a nonlinear SPDEs,

$$dU = (AU + F(U))dt + BdW, \tag{5.13}$$

where $F(U)$ is a mildly nonlinear functions, for example Lipschitz in U, and BdW noise similar to the examples above. We assume that B is a linear operator on the Hilbert space H where U lives, and A generates a strongly continuous semi-group on H. Then there exists a solution operator $S(t)$ of the deterministic nonlinear equation and given some conditions of $S(t)$ we can prove the existence of an invariant measure, see [51], so the above results apply to the nonlinear equation. Thus the SOC theory exists and is similar for nonlinear equations with mild nonlinearities. (Unfortunately, the nonlinearities in the landsurface equations (4.1) and (4.2) are not mild.) However, we expect more complicated SOC systems to exist. The stationary states that we get are not complex, see Definitions 3.1.1 and 3.1.3. The measures on the infinite dimensional spaces that we are getting are all (colored) Gaussian and are completely determined by their mean and variance (the variogram). There must be many spatially complex SOC systems

with more complicated invariant measures, or in other words with rainbow-colored stationary states, so that the higher moments exhibit different spatial scalings.

5.1.2 More General Landsurfaces

In this paper we use the one-dimensional analysis of the water flow over evolving landsurfaces in [78] and [9], based on [26], [50], [66] and [9], to find the coloring of the nonlinear sediment flow, linearized about three stages of evolving landsurfaces. These are the channelizing surface, the adolescent surface and the mature surface. We concluded that the color of the water determines the color of the surfaces. This was done for one particular model of water and sediment flow describing a transport limited situation found in desert environments. For this model we can completely describe the ranges, see [22, 18, 19, 20] in Hack's law, see [10] and [9].

The detachment-limited case must be included to get a more complete stochastic theory of landsurface evolution. Here one waits for the rock to weather before the sediment is carried away. It is probable that the chemical composition of the rock will play a role in the statistical characterization of the system and some results indicate that this is the case at least in the characterization of the temporal evolution. Vegetation cover and soil must also be taken into account, tectonic uplift and diffusion and at high altitudes and in cold climate, the action of glaciers. It is probable that the inclusion of these phenomena will lead to stationary states characterized by more a complex invariant measure than those above, thus producing a more complete stochastic theory of complex SOC systems, with complex stationary states. Indeed studies of DEMs show that topography exhibits fractal; see Klinkenberg and Goodchild [40], and multi-fractal; see Lavallée, Lovejoy and Schertzer [43], structure.

5.2 Conclusions

The stochastic theory of transport-limited landsurfaces identifies three processes that shape eroding surfaces consisting of loose sediment. The first process called the Channelization Process is an infinite-dimensional Brownian motion driven by noise that is white both in time and in its spatial distribution. This process consists of the transient of a random walk biased in the downslope direction. It then saturates in a stationary state characterized by the spatial scaling of Brownian motion. The process is completely characterized by its mean and variance that allow us to compute the variogram of topography. This process channelizes the originally smooth surface and lays down the basic network of streams and rivers. It possess an invariant measure living on the whole of infinite dimensional phase space and is not a SOC system.

The second process is called the Adolescence Process and characterizes the evolution of young surfaces from a convex to a concave shape. This process is driven by colored noise created by shocks, bores and hydraulic jumps, in the water flow and knick points in the sediment flow. The noise is quenched by absence of water a various locations on the surface and pinned by the vanishing of the slope of the water surface. The Adolescence Process is characterized by its mean and variance. It has a stationary state with a spatial roughness coefficient $\chi = 0.66$. It also possesses a colored invariant measure characterizing the stationary state. This makes the Adolescence Process an SOC process.

The third process called the Maturation Process is driven by highly colored noise. It is also characterized by its mean and variance and the variogram scales initially with several characteristic temporal exponents. Eventually it reaches a steady state where the spatial scaling has a large exponent 0.75, indicating a long range correlation. The Maturation Process possesses an invariant measure living on an infinite-dimensional subspace of the original phase space. This measure completely characterizes the stationary state. These properties make the Maturation Process a SOC process with complex temporal transients.

Together these two processes produce the observable properties of transport-limited surfaces, such as Horton's relations and Hack's law, see [10], they possess the numerically observed scaling laws [10] and agree with values obtained form DEMs [77].

SOC systems in Definition 3.1.1 capture the basic properties of self-organized-critical system. The idea of temporal self-organization during the transients is manifested in the magnification of the initially white noise, during a very short initial period of exponential growth and then saturation and coloring by nonlinearities. This is the defining property of these systems. Thus the self-organization is expressed in the spatial structure of the stationary state that is formed by magnification and coloring of small white noise during the transients. The motion is simply projected onto an infinite-dimensional subspace during the transients and the invariant measure living on this subspace determines all the properties of the stationary state. The invariant measure seems the capture the idea of an SOC "attractor" whereas the real attractor of at least the transport-limited landsurfaces is trivial (a flat plateau). Thus SOC systems are defined as systems that color themselves using the white noise in the environment as a source, can show multi-fractal transients and then project onto an infinite-dimensional subspace where they possess an invariant measure completely determining their "critical" stationary state. It is likely that more complex landsurfaces will in addition be shown to have stationary states that themselves are multi-fractal.

Acknowledgments The first and the last authors were supported by grants numbers BCS-9819095, DMS-0072191 and DMS-0352563 from the National Science Foundation whose support is gratefully acknowledged. They also thank Kim Sneppen, Daniel Lavallée, Jonathan Mattingly, Andrea Bertozzi and Edward Welsh for helpful suggestions and Russel Schwab and Kirsten Meeker who redid and added to the simulation on the cluster of workstations, funded by a National Science Foundation SCREMS grant number DMS-0112388, and wrote the programs analyzing the numerical data. This paper was written while the first author was on a sabbatical

at the University of Granada, Spain, whose support is also gratefully acknowledged.

Bibliography

[1] Howard A.D. Theoretical model of optimal drainage networks. *Water Resources Research,* 26:2107–2117, 1990.

[2] Howard A.D. A detachment-limited model of drainage basin evolution. *Water Resources Research,* 30:2261–2285, 1994.

[3] P. Bak. *How nature works : the science of self-organized criticality*. Springer-Verlag, Copernicus, New York, 1996.

[4] P. Bak and M. Paczuski. Complexity, contingency, and criticality. *Proceedings of the National Academy of Science,* 92:6689–6696, 1995.

[5] P. Bak, C. Tang, and K. Wiesenfeld. Self-organized criticality: An explanation of 1/f noise. *hys. Rev. Lett.,* 59:381–384, 1987.

[6] P. Bak, C. Tang, and K. Wiesenfeld. Self-organized criticality. *Physical Review A,* 38:364–374, 1988.

[7] J. R. Banavar, F. Colaiori, A Flammini, A. Giacometti, A. Maritan, and A. Rinaldo. Sculpting of fractal river basin. *Phys. Rev. Lett.,* 78:4522–25, 1997.

[8] A. L. Barabasi and H. E. Stanley. *Fractal Concepts in Surface Growth*. Cambridge Univ. Press, 1995.

[9] B. Birnir. Turbulent rivers. *Submitted to Comm. Pure and Appl. Math.*, 2006.

[10] B. Birnir, T.R. Smith, and G. Merchant. The Scaling of Fluvial Landscapes. *Computers and Geoscience*, 27:1189–1216, 2001.

[11] B. Birnir, T.R. Smith, and G.E. Merchant. Scaling laws and the emergence of channelized drainage patterns in a class of non-linear landscape evolution models. *Proceedings, American Geophysical Union Chapman Conference on Fractal Scaling, Non-linear Dynamics, and Chaos in Hydrologic Systems*, 1998.

[12] Sinclair D. and R.C.Ball. Mechanism for global optimization of river networks from local erosion rules . *Physical Review Letters*, 76:3360–3363, 1996.

[13] D. Dawson. Stochastic evolution equations and related measure processes. *J. Mult. Anal.*, 5:1–52, 1975.

[14] D. A. Dawson and H. Salehi. Spatially homogeneous random evolutions. *J. Multiv. Anal.*, 210:141–180, 1980.

[15] D. Dhar. The abelian sandpile and related models. *Physica A*, 263:4, 1999.

[16] D. Dhar. Studying self-organized criticality with exactly solved models. *cond-mat*, 9909009, 1999.

[17] D. Dhar and P. K. Mohanty. Generic sandpile models have directed percolation exponents. *Phys. Rev. Lett.*, 89:5, 2002.

[18] P. S. Dodds and D. Rothman. Geometry of river networks. I. scaling, fluctuations and deviations. *Phys. Rev. E*, 63:016115, 2000.

[19] P. S. Dodds and D. Rothman. Geometry of river networks. II. distributions of component size and number. *Phys. Rev. E*, 63:016116, 2000.

[20] P. S. Dodds and D. Rothman. Geometry of river networks. III. characterization of component connectivity. *Phys. Rev. E*, 63:016117, 2000.

[21] P. S. Dodds and D. H. Rothman. Unified view of scaling laws for river networks. *Phys. Rev. E.*, 59:4865–77, 1999.

[22] P. S. Dodds and D. H. Rothman. Scaling, universality and geomorphology. *Annu. Rev. Earth Planet Sci.*, 28:571–610, 2000.

[23] Loewenherz-Lawrence D.S. Stability and the initiation of channelized surface drainage: a reassessment of the short wavelength limit . *Journal of Geophysical Research*, 96:8453–8464, 1991.

[24] Loewenherz-Lawrence D.S. Hydrodynamic description for advective sediment transport processes and rill initiation. *Water Resources Research*, 30:3203–3212, 1994.

[25] R. Durrett. *Lecture Notes on Particle Systems and Percolation*. Wadsworth, Belmont, 1988.

[26] S.F. Edwards and D.R. Wilkinson. The surface statistics of a granular aggregate. *Proc. Roy. Soc. London. Series A*, 1982.

[27] Ijjasz-Vasquez E.J., Bras R.L., Rodriguez-Iturbe I., Rigon R., and A. Rinaldo. Are river basins optimal channel networks. *Advances in Water Resources*, 16:69–79, 1993.

[28] V. Frette, K. Christensen, A. Malthe-Sorenssen, J. Feder, T. Jssang, and P. Meakin. Avalanche dynamics in a pile of rice. *Nature*, 379:49–52, 1996.

[29] Willgoose G. A physical explanation for an observed area-slope-elevation relationship for catchments with declining relief. *Water Resources Research*, 30:151–159, 1994.

[30] Willgoose G., Bras R.L., and I. Rodriguez-Iturbe. A coupled channel network growth and hillslope evolution model, 1, theory. *Water Resources Research*, 27:1671–1684, 1991.

[31] Willgoose G., Bras R.L., and I. Rodriguez-Iturbe. A coupled channel network growth and hillslope evolution model, 2, nondimensionalization and applications. *Water Resources Research*, 27:1685–1696, 1991.

[32] A. Giacometti, A. Maritan, and J.R. Banavar. Continuum model for river networks. *Physical Review Letters*, 75:577–580, 1995.

[33] B. Gutenberg and C. F. Richter. Earthquake magnitude, intensity, and acceleration. *Bull. Seismol. Soc. Am.*, 3:163–191, 1942.

[34] J. Hack. Studies of longitudinal stream profiles in Virginia and Maryland. *U.S. Geological Survey Professional Paper 294-B*, 1957.

[35] H. J. Herrmann. Statistical models for granular materials. *Physica A*, 263:51–62, 1957.

[36] N. Izumi and G. Parker. Inception of channelization and drainage basin formation: upstream-driven theory. *J. Fluid Mech.*, 283:341–63, 1995.

[37] Kirkby M. J. A 2-dimensional simulation model for slope and stream evolution . *Hillslope Processes, edited by A. D. Abrahams, Allen and Unwin, Winchester, MA*, pages 203–222, 1986.

[38] M. Kardar, G. Parisi, and Y.-C. Zhang. Dynamic scaling at finite temperatures. *Physical Review Letters*, 56:889, 1986.

[39] T. Kato. *Perturbation Theory for Linear Operators*. Springer, New York, 1966.

[40] B. Klinkenberg and M. Goodchild. The fractal properties of topography. *Earth Surf. Processes Landforms*, 17:217–234, 1992.

[41] J. Krug and H. Spohn. *Kinetic Roughening of Growing Surfaces*. Solids far from Equilibrium, ed. C. Godreche. Cambridge Univ. Press, 1991.

[42] P. La Barbera. Invariance and scaling properties in the distributions of contributing area and energy in drainage basins. *Hydrological Processes*, 8:125–135, 1994.

[43] D. Lavallée, S. Lovejoy, D. Schertzer, and P. Ladoy. Nonlinear variability of landscape topography: Multifractal analysis and simulation. *Fractals in Geometry, edited by N. S. Lam and L. De Cola Prentice Hall, Englewood Cliffs, NJ*, pages 158–192, 1993.

[44] L. Leopold, M. Wolman, and J. Miller. Fluvial processes in geomorphology. 1964.

[45] T.M. Liggett. *Interacting Particle Systems*. Springer, New York, 1985.

[46] B.B. Mandelbrot. *The Fractal Geometry of Nature*. Freeman, New York, New York, 460 pp., 1983.

[47] G. E. Merchant. An elementary theory of drainage basin evolution. University of California, Santa Barbara, Department of Geography, Ph.D thesis, 2000.

[48] B.I. Nikora and V.B. Sapozhnikov. River network fractal geometry and its computer simulation. *Water Resources Research*, 29:3569–3575, 1993.

[49] M. Paczuski. Dynamic scaling: Distinguishing self-organized from generically critical systems. *Physical Review E*, 52:2137–2140, 1995.

[50] G. Parisi. On the spectrum of the one dimensional string. *Europhys. Lett.*, 17:673, 1992.

[51] G. Da Prato and J. Zabczyk. *Ergodicity for Infinite Dimensional Systems*. Cambridge University Press, Cambridge UK, 1996.

[52] W.H. Press. Flicker noise in astronomy and elsewhere. *Comments Astrophys.*, 7:103–119, 1978.

[53] Horton R.E. Erosional development of streams and their drainage basins: a hydrophysical approach to quantitative morphology . *Geol. Soc. Am. Bull.*, 56:275–370, 1945.

[54] A. Rinaldo, I. Rodriguez-Iturbe I., Rinaldo A., Rigon R., Bras R.L., Ijjasz-Vasquez E., and Marani A. Minimum energy and fractal structures of drainge networks. *Water Resources Research*, 28:2183–2195, 1992.

[55] I. Rodriguez-Iturbe, E.J. Ijjasz-Vasquez, and R.L. Bras. Power law distributions of discharge mass and energy in river basin. *Water Resources Research*, 28:1089–1093, 1992.

[56] I. Rodriguez-Iturbe and A. Rinaldo. *Fractal River Basins: Chance and Self-Organization.* Cambridge University Press, Cambridge, 547 pp., 1997.

[57] I. Rodriguez-Iturbe, A. Rinaldo, R. Rigon, R.L. Bras, A. Marani, and E. Ijjasz-Vasquez. Energy dissipation, runoff production, and the three-dimensional structure of river basins. *Water Resources Research*, 28:1095–1103, 1992.

[58] Kramer S. and M. Marder. Evolution of river networks. *Physical Review Letters*, 68:205–208, 1992.

[59] V.B. Sapozhnikov and E. FouFoula-Georgiou. Do current landscape evolution models show self-organized criticality. *Water Resources Research*, 32:1109–1112, 1996.

[60] V.B. Sapozhnikov and E. FouFoula-Georgiou. Self-affinity in braided rivers. *Water Resources Research*, 32:1429–1439, 1996.

[61] V.B. Sapozhnikov and E. FouFoula-Georgiou. Experimental evidence of dynamic scaling and indications of self-organized criticality in braided rivers. *Water Resources Research*, 33:1983–1991, 1997.

[62] A.E. Scheidegger. A stochastic model for drainage patterns in an intermontane trench. *Bulletin of the International Association of Hydrologists*, 12:15–20, 1967.

[63] R.L. Shreve. Statistical law of stream numbers. *Journal of Geology*, 74:17–37, 1966.

[64] R.L. Shreve. Infinite topologically random channel networks. *Journal of Geology*, 75:178–186, 1967.

[65] T.R. Smith, G.E. Merchant, and B. Birnir. Transient attractors: towards a theory of the graded stream for alluvial and bedrock channels. *Computers and Geosciences*, 26(5):531–541, 2000.

[66] K. Sneppen. Self-organized pinning and interface growth in random medium. *Phys. Rew. Lett.*, 69(24), 1992.

[67] K. Sneppen. Fractals and intermittancy in dynamics of large systems. *Nordic Institute for Theoretical Physics, preprint*, 1998.

[68] H. Takayasu. Statistical models of river networks. *Phys. Rev. Lett.*, 63:2563–65, 1989.

[69] D.G. Tarboton, R.L. Bras, and I. Rodriguez-Iturbe. The fractal nature of river networks. *Water Resources Research*, 24:1317–1322, 1988.

[70] D.G. Tarboton, R.L. Bras, and I. Rodriguez-Iturbe. Scaling and elevation in river networks. *Water Resources Research*, 25:2037–2051, 1989.

[71] Smith T.R., B. Birnir, and G.E. Merchant. Towards an elementary theory of drainage basin evolution: I. The theoretical basis. *Computers and Geoscience*, 23(8):811–822, 1997.

[72] Smith T.R. and F.P. Bretherton. Stability and the conservation of mass in drainage-basin evolution . *Water Resources Research*, 8:1506–1529, 1972.

[73] Smith T.R. and G.E. Merchant. Conservation principles and the initiation of channelized surface flows. *in Natural and Anthropomorphic Influences in Geomorphology, ed. J. Costa, A. J. Miller, K. W. Potter, and P. Wilcock*, pages 1–25, 1995.

[74] Smith T.R., G.E. Merchant, and B. Birnir. Towards an elementary theory of drainage basin evolution: II. A computational evaluation. *Computers and Geoscience*, 23(8):823–849, 1997.

[75] Ivashkevich E. V. and Priezzhev V. B. Introduction to the sandpile model. *Physica A*, 254:97, 1998.

[76] J. B. Walsh. *An introduction to stochastic partial differential equations*. Springer Lecture Notes, eds. A. Dold and B. Eckmann. Springer, New York, New York, 1984.

[77] J.K. Weissel, L.F. Pratson, and A. Malinverno. The length-scaling of topography. *Journal of Geophysical Research*, 99:13997–14012, 1994.

[78] E. Welsh, B. Birnir, and A. Bertozzi. Shocks in the evolution of an eroding channel. 2005. Submitted.

[79] E. W. Welsh. Landscape erosion: Convergence, singularities and shocks in a continous transport-limited model. Duke University, Department of Mathematics, Ph.D thesis, 2003.

[80] J.C. Willis. Fractals and power laws in biology, sociology, and physics. *Nature*, February:178, 1924.

[81] K. Yosida. *Functional Analysis*. Springer Verlag, New York, 1980.

[82] G.K. Zipf. *Human Behavior and the Principle of Least Effort*. Addison-Wesley, Cambridge, MA, 573 pp., 1949.